



**Università degli Studi di Padova**

---

**DIPARTIMENTO DI INGEGNERIA INDUSTRIALE**

*Corso di Laurea Magistrale in Ingegneria Aerospaziale*



**Study of the performance of a  
racing motorcycle by the optimal  
maneuver method**

*Laureando*

**Andrea Menardo**

*Relatore*

**Prof. Vittore Cossalter**

*Co-relatore*

**Prof. Matteo Massaro**



*Alla mia  
Famiglia*



# Contents

<b>Introduction</b>	<b>ix</b>
<b>1 Optimal Maneuver Method</b>	<b>1</b>
1.1 Vehicle manoeuvrability and handling . . . . .	1
1.2 The Optimal Control Problem . . . . .	1
1.2.1 Solution of the optimal control problem . . . . .	2
1.2.2 Optimal Maneuver Method: dynamic optimization for continuous system . . . . .	3
1.2.3 Track and Maneuver Description . . . . .	6
1.2.4 Boundary conditions . . . . .	7
<b>2 Mathematical Model</b>	<b>9</b>
2.1 Dynamic Model . . . . .	9
2.2 Suspension Model . . . . .	10
2.3 Engine data . . . . .	11
2.4 Penalties and boundary conditions . . . . .	11
2.5 Launching process simulation . . . . .	12
2.6 LaunchSims.exe . . . . .	15
<b>3 Track reconstruction</b>	<b>19</b>
<b>4 Model Validation</b>	<b>23</b>
4.1 Comparison between Simulation and Telemetry . . . . .	24
4.1.1 Velocity comparison: Telemetry vs. Simulation . . . . .	24
4.1.2 Gear shifting comparison: Telemetry vs. Simulation . . . . .	25
4.1.3 Roll angle comparison: Telemetry vs. Simulation . . . . .	26
<b>5 Analysis of a Racing Motorcycle</b>	<b>29</b>
5.1 Gear shifting analysis . . . . .	30
5.2 New throttle body analysis . . . . .	33
5.2.1 New throttle body vs old throttle body . . . . .	33
5.2.2 Considerations . . . . .	35
5.3 New gearing set analysis . . . . .	36
5.3.1 Summary . . . . .	36
5.3.2 Simulation results . . . . .	39
5.3.3 Considerations . . . . .	43

<b>6 Parametric analysis</b>	<b>45</b>
6.1 Influence of the sprocket-pignon ratio . . . . .	45
6.2 Influence of the centre of mass position . . . . .	48
6.3 Influence of Roll and Yaw inertia . . . . .	50
6.4 Influence of the aerodynamic drag . . . . .	50
<b>Conclusions</b>	<b>55</b>
<b>Bibliography</b>	<b>59</b>







# Introduction

The Optimal Maneuver Method is a package for optimal control problem simulations developed by the Motorcycle Dynamics Research Group of the University of Padova and by the University of Trento. This methodology has been employed in the last ten years as an advanced tool for the evaluation of manoeuvrability of motorcycles and cars, which is an intrinsic property of the vehicle, the second is the judgement of the driver to find different vehicles more or less easy to drive.

The method is based on the mathematical formulation (TPBVP) of a vehicle model capable of getting the dynamics of the system and on the concept of ideal rider, or rather the best driver capable of employing the vehicle at its maximum potential in every situation.

It is a tool developed expressly for vehicle dynamics and provides for minimum time simulations of a vehicle, subject to some physical limitations (e.g. boundaries of the track, maximum available power, tire adherence etc.), that has to travel from a starting point to a final one within a whole track or a specific part of the track.

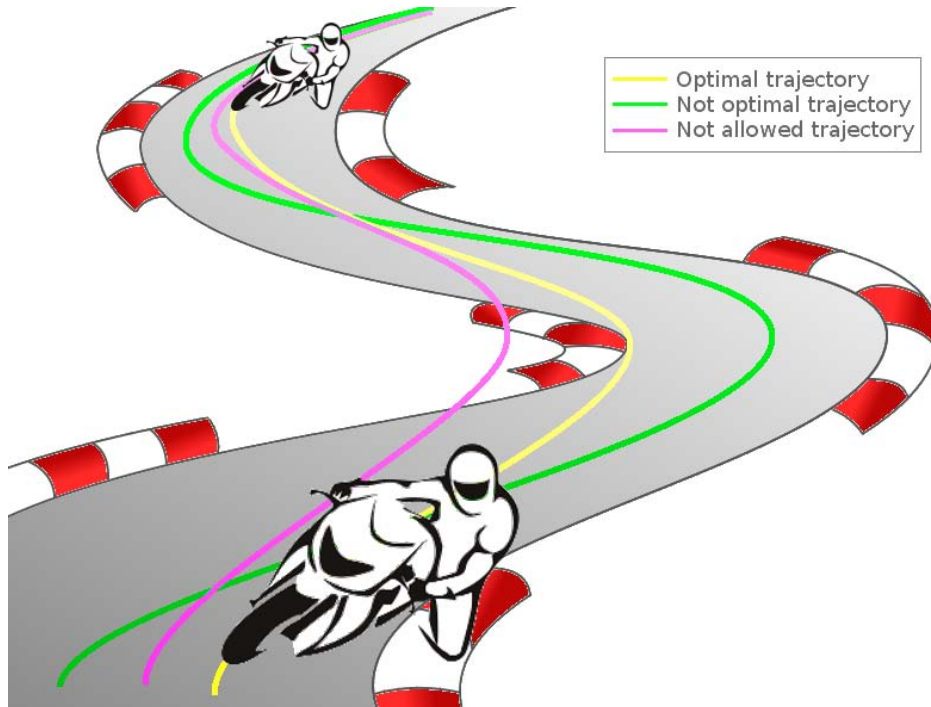


Figure 1: Example: optimal maneuver trajectories

The result of this optimization are, in terms of state variables of the systems, the optimal trajectory of the vehicle on the track and the input to give as controls to the vehicle in order to obtain the optimal trajectory (as roll angle, steering angle, speed, etc.). Other output are available, so it is easy to calculate any parameters of interest. In this thesis, the optimal control problem is used only with the dynamics of motorcycle, but it is possible apply it to different models, (as road vehicle, go-kart, rally car, formula 1, etc.) without changing the treatment of the problem (the dynamic must be relevant to the type of vehicle). In aerospace field, some possible uses of the optimal control problem are fuel efficiency for commercial flights and orbital maneuvers. It is known to all how important it is to identify the route, which minimizes the fuel to take on board, which translates into an economic saving for the flight company. The same considerations can be made for the orbital maneuvers, to organize what are the best strategies to use fuel (for example, in the docking manoeuvres or attitude control) or for planning the trajectory, in a collaborative way between drones and rover.

In this thesis, the software has been used as an advanced tool for the preliminary study, as method of comparison with the telemetry and as strategy planner lap. The first part will be explained how the software mathematically works, which models are used and the limits of them (the dynamics of the motorcycle model will not be treated).

A second part where it will be treated as configure the tool to be calibrated specifically for the purpose required to avoid false results. An important aspect of it is the convergence of the problem; it is not always guaranteed and will then explain what to do when this happens. After that will demonstrate how you can make comparisons between results of simulations and real data from telemetry. It will also be shown what considerations can be drawn, and how this can lead to different strategies lap, for example the use of a gear rather than another.

A third part, we will see how it is possible to use the software as a tool for the development of a new engine or a part of it. It is a means to see if further changes or is currently leading to a benefit on a particular track and / or more tracks. In other words, it can be used to see if the way taken is the right one. It is better to point out right away that to achieve the goal of this last part is required confidence of the software that currently there is not. It needs further development to become a reliable tool, it is essentially a possible future use and how it could become indispensable because the trend of recent years is to decrease the test track. Another advantage is to discover such problems before you even get on the track.

Finally, parametric analysis has been done to improve the performance of the

motorcycle by acting on other parameters, such as the centre of mass position and drag. For the latter part, it has been taken to a reference configuration and the parameters varied in a specific proportion, however, was not possible to compare the results of the simulations with the track tests. This tool is used as an analysis before arriving at the track, so as to make only small adjustments during the race weekend and also allows assessing driver skills.



# Chapter 1

---

## Optimal Maneuver Method

### Introduction

The Optimal Maneuver Method consist in the solution of a two-point control boundary value problem, in which a vehicle, subject to physical constraints like tyre adherence and road borders among others, is driver's actions that make the vehicle move between the two states in the most efficient way are found as a part of the solution procedure and represent the actions of a sort of ideal, perfect driver. The resulting motion is called the *optimal maneuver*.

### 1.1 Vehicle manoeuvrability and handling

Before entering into the mathematical details of the method we are going to explain better the concept of *manoeuvrability* and *handling*.

**Manoeuvrability:** is the ability of a vehicle to complete a maneuver as fast as possible and without exceeding existing physical limitations like tyre adherence or road boarders.

**Handling:** is the judgement of the driver to find different vehicles more or less easy to drive.

**Maneuver:** is a generic motion between given initial and final positions or states. During the motion the vehicle must respect some trajectory constraints, which means that some states are not allowed, like lane borders.

### 1.2 The Optimal Control Problem

In order to evaluate manoeuvrability, the motion of the vehicle needs to be given  $\mathbf{x}(t)$  function of system state and  $\mathbf{u}(t)$  control inputs, must be known. There are many acceptable solutions of the equations of motion, each being produced by a different choice of control inputs  $\mathbf{u}(t)$  and representing a different possible way of completing the same maneuver. Of all these solutions

however, only one minimises the penalty and represents the most efficient way to do the maneuver. This special solutions is called the *optimal maneuver*.

We need to find inputs  $\mathbf{u}(t)$  such that the penalty given is minimised subject to the following constraints:

1. Equations of motion:

$$\mathbf{F}(\mathbf{x}, \dot{\mathbf{x}}, \mathbf{u}, t) = 0 \quad (1.1)$$

2. Boundary conditions:

$$\begin{aligned} \Psi'_j(\mathbf{x}(0)) &= 0 & j=1, m' \\ \Psi''_j(\mathbf{x}(T)) &= 0 & j=1, m'' \end{aligned} \quad (1.2)$$

3. Trajectory constraints:

$$\Phi_i(\mathbf{x}, \mathbf{u}, t) < 0 \quad i=1, m \quad (1.3)$$

For simplicity we assumed that the final time  $T$  is fixed. The last equation is changed with the penalty function by adding additional terms that apply a large penalty if inequality constraints are violated. We thus use the following:

$$I = \int_0^T \left\{ f_0(\mathbf{x}, \mathbf{u}, t) + \sum_{i=1}^m w f_i(\mathbf{x}, \mathbf{u}, t) \right\} dt \quad (1.4)$$

where  $w f_i(\mathbf{x}, \mathbf{u}, t)$  are weighting functions that take on a large value (compared to  $f_0$ ) if corresponding constraints  $\Phi_i(\mathbf{x}, \mathbf{u}, t)$  are violated, and are instead negligible if constraints are not violated. The use of this equation instead of inequality is clearly a practical solution.

### 1.2.1 Solution of the optimal control problem

The solution of the optimal control problem formed by equations of motion, boundary conditions and the penalty function modified may be reduced to the solution of a system of ordinary differential equations with boundary conditions. The system are solved by symbolic algebra software that automatically produce the include files that encode the various terms of the expressions.

### 1.2.2 Optimal Maneuver Method: dynamic optimization for continuous system

Optimal control aims at minimizing a certain cost function (as show above) subject to a certain number of equality and/or inequality constraints. Given a continuous dynamic system

$$\dot{\mathbf{x}} = \mathbf{f}[\mathbf{x}(t), \mathbf{u}(t)] \quad (1.5)$$

with initial conditions:

$$\mathbf{x}(t_0) = \mathbf{x}_0 \quad (1.6)$$

the problem is to find the sequence of control vector  $\mathbf{u}$  to minimize a certain performance index:

$$J = \phi[\mathbf{x}(t_f)] + \int_{t_0}^{t_f} L[\mathbf{x}(t), \mathbf{u}(t)] dt \quad (1.7)$$

subject to the equality Eq.1.5 and Eq. 1.6. The constraints 1.5 and 1.6 are the adjoin to the performance index 1.7 through the use of Lagrange multipliers  $\lambda$ :

$$\bar{J} = \phi + \int_{t_0}^{t_f} \{L[\mathbf{x}(t), \mathbf{u}(t)] + \boldsymbol{\lambda}^T(t)[\mathbf{f}[\mathbf{x}(t), \mathbf{u}(t)] - \dot{\mathbf{x}}]\} dt \quad (1.8)$$

Defining the Hamiltonian H as:

$$H(t) = L(t) + \boldsymbol{\lambda}^T(t)[\mathbf{f}[\mathbf{x}(t), \mathbf{u}(t)]] \quad (1.9)$$

Eq.1.8 can be rewritten as:

$$\bar{J} = \phi + \int_{t_0}^{t_f} [H(t) - \boldsymbol{\lambda}^T(t)\dot{\mathbf{x}}] dt \quad (1.10)$$

that correspond to:

$$\bar{J} = \phi + \int_{t_0}^{t_f} H(t)dt - \int_{t_0}^{t_f} \boldsymbol{\lambda}^T(t)\dot{\mathbf{x}}dt \quad (1.11)$$

Now integrating by parts the second integral:

$$\bar{J} = \phi + \int_{t_0}^{t_f} H(t)dt - \left\{ [\boldsymbol{\lambda}^T(t)\mathbf{x}(t)]_0^{t_f} - \int_{t_0}^{t_f} \dot{\boldsymbol{\lambda}}^T(t)\mathbf{x}(t)dt \right\} \quad (1.12)$$

and thus:

$$\bar{J} = \phi - \boldsymbol{\lambda}^T(t_f)\mathbf{x}(t_f) + \int_{t_0}^{t_f} \left[ H(t) + \dot{\boldsymbol{\lambda}}^T(t)\mathbf{x}(t) \right] dt + \boldsymbol{\lambda}^T(t_0)\mathbf{x}_0 \quad (1.13)$$

The necessary condition for a stationary solution for arbitrary  $\delta u$  is reduced to solve  $d\bar{J} = 0$ :

$$\begin{aligned} d\bar{J} = & [\boldsymbol{\phi}_x - \boldsymbol{\lambda}^T(t_f)] d\mathbf{x}(t_f) + \boldsymbol{\lambda}^T(t_0)d\mathbf{x}_0 + \\ & + \int_{t_0}^{t_f} \left\{ [\mathbf{H}_x(\mathbf{t}) + \dot{\boldsymbol{\lambda}}^T(t)] \delta\mathbf{x} + \mathbf{H}_u(t)\delta\mathbf{u} \right\} dt = 0 \end{aligned} \quad (1.14)$$

where  $\boldsymbol{\phi}_x$  is the gradient of  $\phi$  respect to  $x$ , while  $\mathbf{H}_x$  and  $\mathbf{H}_u$  are the gradient of  $H$  respect to  $x$  and  $u$  respectively. Solving the Eq.1.14 corresponds to the solution of the following set of equations:

$$\boldsymbol{\phi}_x - \boldsymbol{\lambda}^T(t_f) = 0 \quad (1.15)$$

$$\boldsymbol{\lambda}^T(t_0) = 0 \quad (1.16)$$

$$\mathbf{H}_x + \dot{\boldsymbol{\lambda}}^T = 0 \quad (1.17)$$



$$\mathbf{H}_u = 0 \quad (1.18)$$

Note that the number of Eq.1.16 corresponds to the number of initial conditions left free in Eq.1.6. In other words, if all initial conditions are set Eq.1.16 is not used, while if all initial conditions are left free Eq.1.16 has the size of the model state vector  $\mathbf{x}$ . Terminal constraints, e.g. to specify the final value of some components of  $\mathbf{x}(t_f)$ , can be added in the form:

$$\psi[\mathbf{x}(t_f)] = 0 \quad (1.19)$$

As a consequence the performance index  $\bar{J}$  in Eq.1.12 is update to include an additional term  $\boldsymbol{\nu}^T \boldsymbol{\psi}$  (where  $\boldsymbol{\nu}$  is the related Lagrange multiplier). When deriving  $d\bar{J}$  the only difference is a new term  $\boldsymbol{\nu}^T \boldsymbol{\psi}_x$  into the first bracket. Therefore Eq.1.15 is update to:

$$\boldsymbol{\phi}_x + \boldsymbol{\nu}^T \boldsymbol{\psi}_x - \boldsymbol{\lambda}^T(t_f) = 0 \quad (1.20)$$

Summarizing, the optimal solution is found by solving the Two Point Boundary Value Problem (TPBVP) defined by the model equations Eq.1.5, free initial states equations Eq.1.16, co-equations Eq.1.17, optimality equations Eq.1.18, initial conditions Eq.1.6 (first point of the TPBVP) and the final conditions Eq.1.20 (second point of the TPBVP). Additional inequality constraint (e.g. those on inputs and those to account for physical limitations during the simulation) are added into the performance index  $J$  Eq.1.8 using penalty functions (soft constraint strategy), thus not changing the problem formulation described. These are functions that assume high values, penalizing the performance index while inequality constraints are violated or at least when they are very closed to zero. Basically a sum of penalty functions is included in the performance index in Eq.1.7.

$$J = \phi[\mathbf{x}(t_f)] + \int_{t_0}^{t_f} L[\mathbf{x}(t), \mathbf{u}(t)] + \sum_{i=1}^q p_i [d_i \mathbf{x}(t), \mathbf{u}(t)] dt \quad (1.21)$$

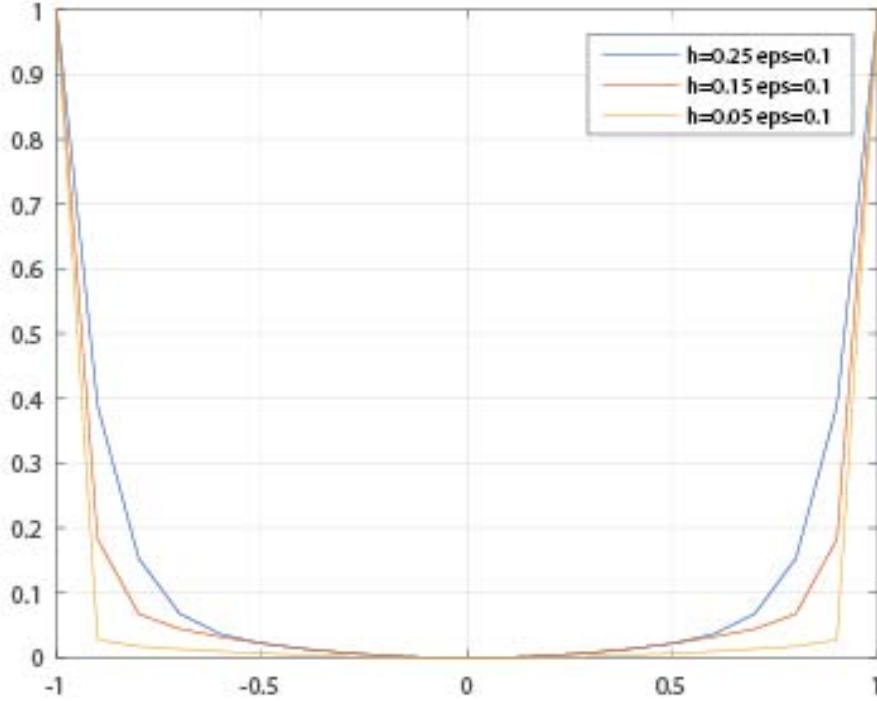


Figure 1.1: Quadratic control penalty for different values of  $h$

where  $p_i$  are penalty functions and  $d_i(\mathbf{x}(t), \mathbf{u}(t))$  are equations that has to be penalized by means of  $p_i$ . Different shapes of these  $p$  functions are possible: once the user has selected the desired function its features are basically settable through a couple of parameters (i.e.  $h$  and  $\epsilon$ ) to adjust the shape of the function itself (1.1).

The resulting algebraic-differential system is discretized in order to obtain a finite dimensional algebraic problem. The simulation interval is split into  $N$  intervals. The resulting system can be solved using a solver for non-linear algebraic equations.

### 1.2.3 Track and Maneuver Description

The position of the vehicle is given in a system of curvilinear coordinates that follow the road lane, rather than by means of absolute coordinates  $x, y$  and absolute yaw  $\Psi$ . The position of the vehicle is defined by curvilinear abscissas  $s_1, s_2$ , the former following the lane centreline, the latter defining the position of the vehicle perpendicular to the centreline. The orientation of the vehicle is

measured from the centreline tangent by angle  $\alpha$  in place of using absolute yaw  $\Psi$ . The choice of curvilinear coordinates makes it easier to formulate initial and final conditions relative to the lane and to define the trajectory constraint that makes the "vehicle stay with lane". In fact, if  $l_2$  represents the half-width of the lane this constraint is written simply as:

$$-l_2 < s_2 < l_2$$

The shape of the road lane is described by given functions  $xc(s_1)$ ,  $yc(s_1)$  that define the centreline as a parametric curve. The transformation from curvilinear coordinates  $s_1, s_2, \alpha$ , and absolute coordinates  $x, y$  and  $\Psi$  is the following:

$$\begin{aligned} x &= xc(s_1) - s_2 \sin(\theta(s_1)) \\ y &= yc(s_1) + s_2 \cos(\theta(s_1)) \\ \Psi &= \theta(s_1) - \alpha \end{aligned} \tag{1.22}$$

The position of the vehicle is obtained by integrating the velocities in the system of curvilinear coordinates  $s_1, s_2, \alpha$ , that result:

$$\begin{aligned} \dot{s}_1 &= \frac{1}{1 - s_2 \sin(\Theta(s_1))} \{u \cos(\alpha) + v \sin(\alpha)\} \\ \dot{s}_2 &= v \cos(\alpha) + u \sin(\alpha) \\ \dot{\alpha} &= \Theta(s_1) \dot{s}_1 - \Psi' \end{aligned} \tag{1.23}$$

More details about how the track was built, will be shown in chapter 3.

#### 1.2.4 Boundary conditions

To complete the description of the maneuver, the initial and final conditions must be given. At the beginning we assign initial position and velocity, leave the initial thrust  $S$  free and assign vertical reactions consistent with it. At the end we leave the final longitudinal position and velocity free so that the travel time may really be minimised as is required by the penalty function. We accept different exit position  $s_2$  but the final direction of travel must be parallel of the centreline.



# Chapter 2

## Mathematical Model

### 2.1 Dynamic Model

The motorcycle dynamic is described in the Maple file. Inside of that, it is possible to find all the details of motorcycle model, the active and reactive forces, the Newton-Euler equations and the tyre model.

A racing motorcycle model is reported in Figure 2.1, on SAE reference system.

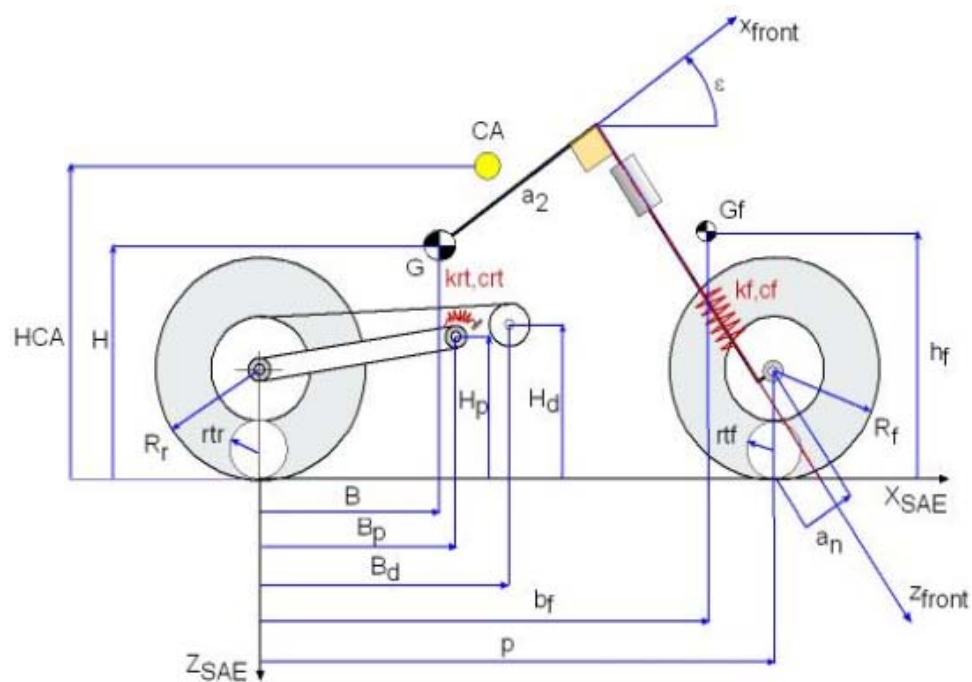


Figure 2.1: Geometry of a racing motorcycle.

where:

- $H$  is the height and  $B$  is the lateral position of the centre of mass  $G$ .
- $H_p$  is the height and  $B_p$  is the lateral position of the swingarm pivot.

- $Hd$  is the height and  $Bd$  is the lateral position of the pignon.
- $hf$  is the height and  $bf$  is the lateral position of the centre of mass of the front assembly  $Gf$ .
- $HCA$  is the height of the centre of the pressure centre  $CA$ .
- $p$  is the wheelbase;
- $\epsilon$  is the caster angle.
- $an$  is the forward offset.
- $R_r$  and  $R_f$  are respectively the rear and the front radius wheel.
- $t_r$  and  $t_f$  are respectively the rear and the front radius of the cross section.
- $krt$  and  $crt$  are stiffness and damping of the rear suspension.
- $kf$  and  $cf$  are stiffness and damping of the front suspension.

The model proposed above is nine degrees of freedom: the speed  $v(t)$ , the sideslip angle  $\lambda(t)$ , the vertical displacement  $z(t)$ , the roll, pitch and yaw angles  $\psi(t)$ ,  $\phi(t)$  and  $\mu(t)$ , the steering  $\delta(t)$ , the linear deformation of the front suspension and torsional deformation of the rear suspension  $zsf(t)$  and  $\theta_s(t)$ . Finally, the input control parameters are the steering torque  $\tau$  and the longitudinal forces  $Sr(t)$  and  $Sf(t)$ .

There are also two files that allow formulating the problem as time variant and optimal control formulation. The discussion of these topics is beyond the scope of this thesis.

## 2.2 Suspension Model

The suspension model is defined by ruby file. It is possible define different forces in order to split the contribution of the rear and the front force independently. The total suspension force due to the both spring and damper elements is introduced in the dynamic model of the vehicle. Let's focus on the spring element, it is define using a fifth degree polynomial function of the displacement  $x$ :

$$F(x) = R_0 + R_1x + R_2x^2 + R_3x^3 + R_4x^4 + R_5x^5 \quad (2.1)$$

where  $x$  is the displacement,  $R_0$  is the spring preload and  $R_1$  is the spring stiffness. We can set to zero  $R_2, R_3, R_4, R_5$  coefficients to obtain a simple linear suspension model. Regarding the damper is define using an "Akima" spline. The procedure involves the reading of certain values of normalized speed which corresponds to a force, obtained for example by testing. These values are used for the creation of the spline.

Finally, the transmission kinematics is also define using a fifth degree polynomial:

$$T_k(x) = a_0 + a_1x + a_2x^2 + a_3x^3 + a_4x^4 + a_5x^5 \quad (2.2)$$

As before, if we set to zero  $a_2, a_3, a_4, a_5$  coefficients to obtain a simple linear transmission kinematics model.

## 2.3 Engine data

The engine model is defined by ruby file. Inside this is defined the configuration of engine and gear set. About the engine is simply loaded the engine revolutions and the output torque, it is also possible multiply by a coefficient in order to adjust the torque available with the effective torque on real engine. The values of the engine revolutions and the output torque are the same that are obtained, for example, by engine test stand. In our case we were provided by the commission team.

Regarding the gear, they are inserted various ratios of each gear, the primary ratio and the number of teeth of the sprocket and pinion. We can define different ratio for each gear which then can be called up with a script that will be shown in section 2.6.

The same applies to the engine, it is possible to define multiple engine configurations to be recalled later.

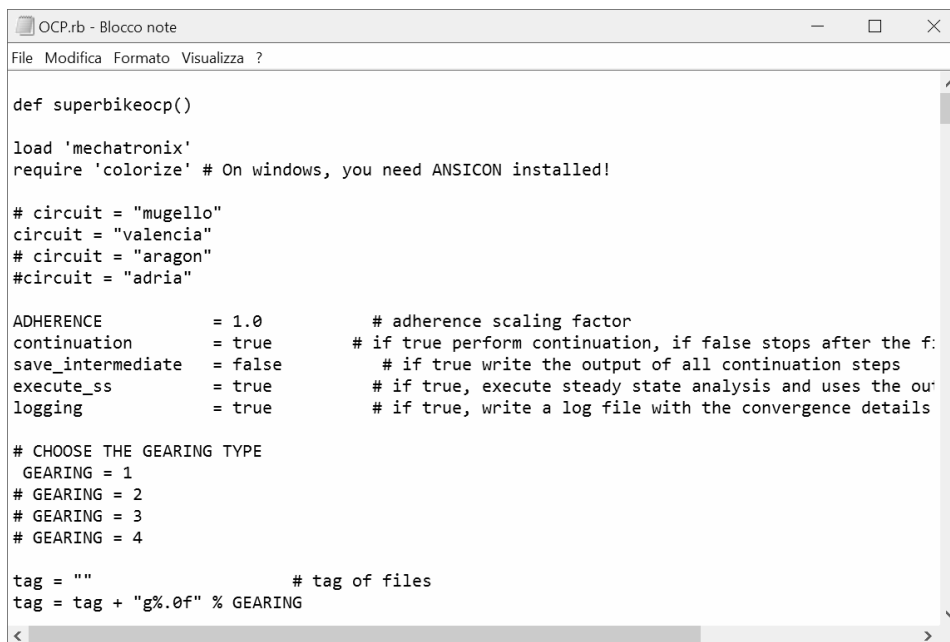
## 2.4 Penalties and boundary conditions

The penalties are introduced in the penalties ruby file. In this file it is possible changed the  $h$  and  $\epsilon$  parameters described in section 1.2.2 for all the penalties. Sometimes it is appropriate to change these values to ensure convergence of the problem, remember that in order to be comparable two or more solutions must be calculated using the same parameters. The same considerations apply for the boundary conditions described in section 1.2.4, which are freely settable in

the ruby file "*Boundary conditions*". Here, we can set *free* if we want to keep out the variable or *set* if we impose a value.

## 2.5 Launching process simulation

This section is intended to provide a guideline on how to configure the files needed to run the software 'xoptima' and how to use it. First, open the *OCP.rb* file in the folder: **XOptimaScripts\data**. To set the desired circuit comment



```

OCP.rb - Blocco note
File Modifica Formato Visualizza ?

def superbikeocp()

load 'mechatronix'
require 'colorize' # On windows, you need ANSICON installed!

# circuit = "mugello"
circuit = "valencia"
# circuit = "aragon"
#circuit = "adria"

ADHERENCE           = 1.0           # adherence scaling factor
continuation         = true          # if true perform continuation, if false stops after the f:
save_intermediate    = false        # if true write the output of all continuation steps
execute_ss           = true          # if true, execute steady state analysis and uses the ou
logging              = true          # if true, write a log file with the convergence details

# CHOOSE THE GEARING TYPE
GEARING = 1
# GEARING = 2
# GEARING = 3
# GEARING = 4

tag = ""              # tag of files
tag = tag + "g%.0f" % GEARING

```

Figure 2.2: Example of *OCP.rb* file

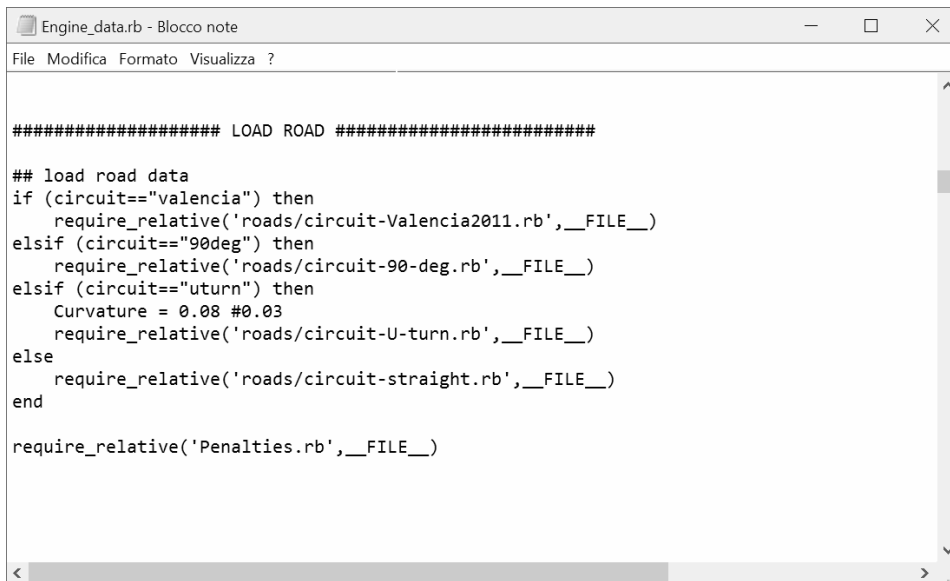
all other circuits with the symbol #, leaving not commented on the circuit chosen (for example, in Fig 2.2 was chosen the Valencia circuit).

Pay attention to have uploaded the ruby file successfully from the folder: **XOptimaScripts\data\roads** and is correctly loaded in the file OCP as shown in Fig.2.3.

How circuits are constructed are explained in Chapter 3.

The same considerations can be made for the gearing as reported in Fig.2.2, to set the desired gearing set comment all other gears with the symbol #. The gearing set are inserted in the *Engine\_data.rb* file in the folder: **XOptimaScripts\data\Moto\_data** as defined in section and as shown below:





```

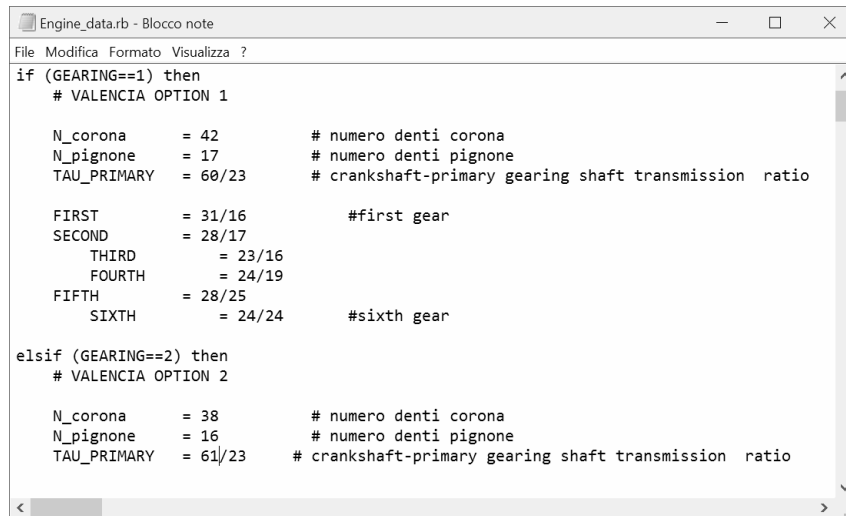
Engine_data.rb - Blocco note
File Modifica Formato Visualizza ?

##### LOAD ROAD #####

## load road data
if (circuit=="valencia") then
  require_relative('roads/circuit-Valencia2011.rb',__FILE__)
elsif (circuit=="90deg") then
  require_relative('roads/circuit-90-deg.rb',__FILE__)
elsif (circuit=="uturn") then
  Curvature = 0.08 #0.03
  require_relative('roads/circuit-U-turn.rb',__FILE__)
else
  require_relative('roads/circuit-straight.rb',__FILE__)
end

require_relative('Penalties.rb',__FILE__)

```

Figure 2.3: Correct load of track in *OCP.rb* file


```

Engine_data.rb - Blocco note
File Modifica Formato Visualizza ?

if (GEARING==1) then
  # VALENCIA OPTION 1

  N_corona      = 42      # numero denti corona
  N_pignone     = 17      # numero denti pignone
  TAU_PRIMARY   = 60/23   # crankshaft-primary gearing shaft transmission ratio

  FIRST         = 31/16   #first gear
  SECOND        = 28/17
  THIRD         = 23/16
  FOURTH        = 24/19
  FIFTH         = 28/25
  SIXTH         = 24/24   #sixth gear

elsif (GEARING==2) then
  # VALENCIA OPTION 2

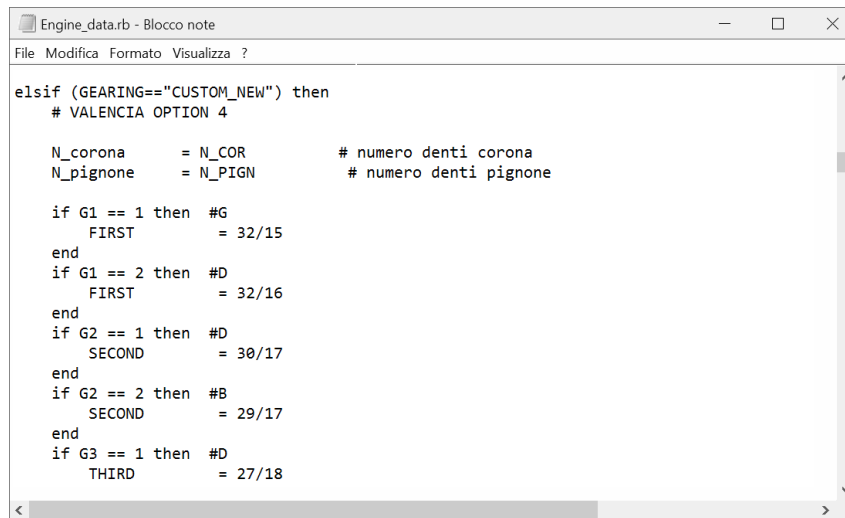
  N_corona      = 38      # numero denti corona
  N_pignone     = 16      # numero denti pignone
  TAU_PRIMARY   = 61/23   # crankshaft-primary gearing shaft transmission ratio

```

Figure 2.4: Example of syntax for gearing set in *Engine\_data.rb* file

In the same file, is possible also define the engine model, changing the values of rpm and torque with the desired ones. An other possibility, is define different gear ratio depending on a parameter (simply through a *if* cycle) which will be explained in the section 2.6.

When configured with all the required parameters, we run the solver.



```

Engine_data.rb - Blocco note
File Modifica Formato Visualizza ?

elseif (GEARING=="CUSTOM_NEW") then
  # VALENCIA OPTION 4

  N_corona      = N_COR      # numero denti corona
  N_pignone     = N_PIGN     # numero denti pignone

  if G1 == 1 then #G
    FIRST      = 32/15
  end
  if G1 == 2 then #D
    FIRST      = 32/16
  end
  if G2 == 1 then #D
    SECOND     = 30/17
  end
  if G2 == 2 then #B
    SECOND     = 29/17
  end
  if G3 == 1 then #D
    THIRD      = 27/18
  end

```

Figure 2.5: Example of *if* cycle for gearing set in *Engine\_data.rb* file

We go on the command prompt, we position in the folder **C:\...\XOptimaScripts**<sup>1</sup> and type the command **mxint mySuperBikeOCP\_run.rb**. If everything is ok, will start a screen, where you see mxint and the solver begins to iterate. You will see the iteration step, the tolerance between the step *i* and the step *i-1* and other parameter (like, lambda). If the required tolerance is reached within a certain limit of iterations, the problem converges. The process is repeated several times in order to refine the final solution. At the end of the entire process, you will appear either *"all done folks"*, i.e. the problem converges or *"solver crash"*, i.e. the problem does not converge. In both cases it will generate a *.txt* file, in the folder **\OCPResults** that loaded on a matlab script allows you to view the simulation results. Let's look at the file matlab, renamed *"plotOCPResults.m"*, shown in Fig.2.6

To select the circuit of interest must remove the comment `%` from the correct line, and leave it in all other. The same for the tag, which represents the configuration of gearing set choice (in Fig.2.6, for example, is select the Valencia's track with configuration of gearing set 'g1'). Note, the file must exist in the current folder set on matlab start screen. Press on "run" button and if all is right, will display the minimum time and various figures related to the trajectory, the speed, the acceleration, the gear shift and more other.

<sup>1</sup>Remember, to open a folder on command prompt use 'cd' following the folder name.

```

34
35 % IMPORT THE FILE
36
37 % SELECT WHICH CIRCUIT
38
39 % circuit = 'straight';
40 % circuit = 'uturn';
41 %circuit = 'road1';
42 - circuit = 'valencia';
43 %circuit = 'mugello';
44 %circuit = 'misano';
45 %circuit = 'vary';
46 %circuit = 'aragom';
47 %circuit = 'Argentina';
48 %circuit = 'oring';
49 %circuit = 'losail_turn';
50
51
52 % SELECT WHICH TAG
53
54 - tag='g1';
55 %tag='g2';
56 %tag='g3';
57 %tag='g4';
58
59 % FILE TO READ
60
61 - fileToRead = ['SuperBikeOCP_',circuit,'_',tag,'.txt'];
62

```

Figure 2.6: Screen of the *plotOCPResults* matlab file

## 2.6 LaunchSims.exe

Launching "*LaunchSims.exe*" the screen that we are facing is to figure 2.7; LaunchSims is an applications that allow to automatically launch simulations and cycling on some parameters, which will be explained below. Let's look at the top left, we note that a ruby file is requested. Here, we load the *OCF* ruby file, which contains the entire procedure required from simulation.

In the bottom box, are thrown into the parameters on which cycling, as the number of teeth of the sprocket, the number of teeth of the pinion, the gear ratio and if required, the engine to use. Just for example, look at the third line  $G1:1:2:1$ , the way to read is this  $G1$  ranging from 1 to 2 with step of one. For the first cycle  $G1 = 1$ , i.e. corresponding to a specific gear ratio, and the other parameter are fixed; for the second cycle  $G1 = 2$  that corresponding to an another specific gear ratio different from previous (as shown in Fig.2.5) and all the other parameter are fixed. By doing so we get all the possible combination and this makes it very convenient to find what is the best configuration of gear that optimizes the performance, such as time lap. On the near box,

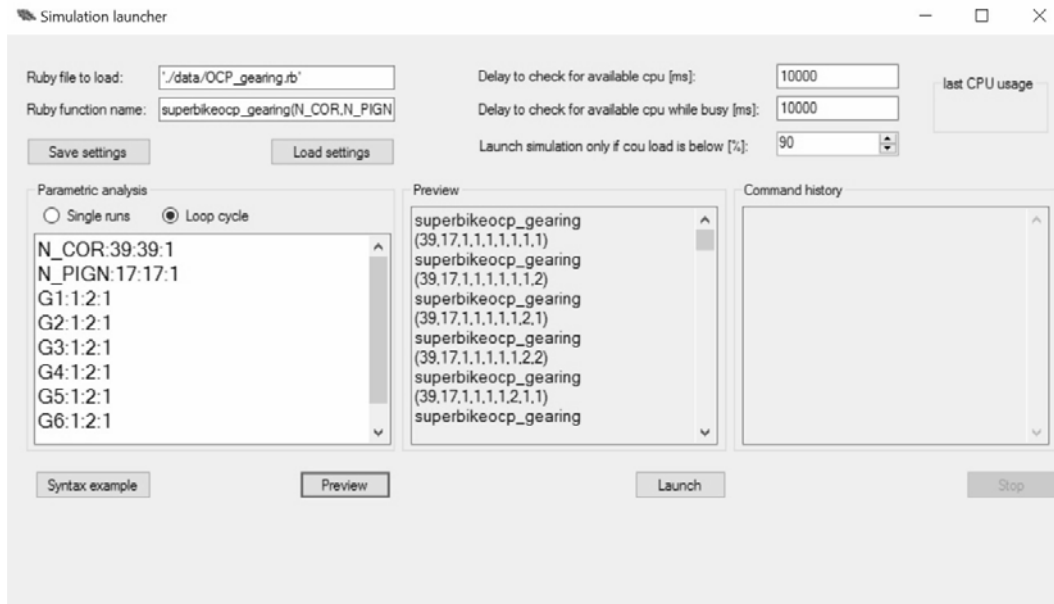


Figure 2.7: Home screen of "Simulation Launcher"

all possible configurations are shown and the next one show which is currently running. Up the command history, the are some windows that allows when the next simulation can running. Once checked in the preview box and sure we do all right, we can click on the launch button. It's possible stop running but the last simulations continue until to the end of process.

The time required for the whole process depends on how well the problem converges, it is frequently likely that some simulations do not converge.





# Chapter 3

## Track reconstruction

During the work of this thesis is not to have happened to some tracks available. The purpose of this chapter is how to rebuild a circuit. First of all, we must have a picture of the track as accurate as possible, if not we can download one from Google Maps, as is proposed in this chapter (we take as reference the circuit of Termas de Río Hondo, Argentina).

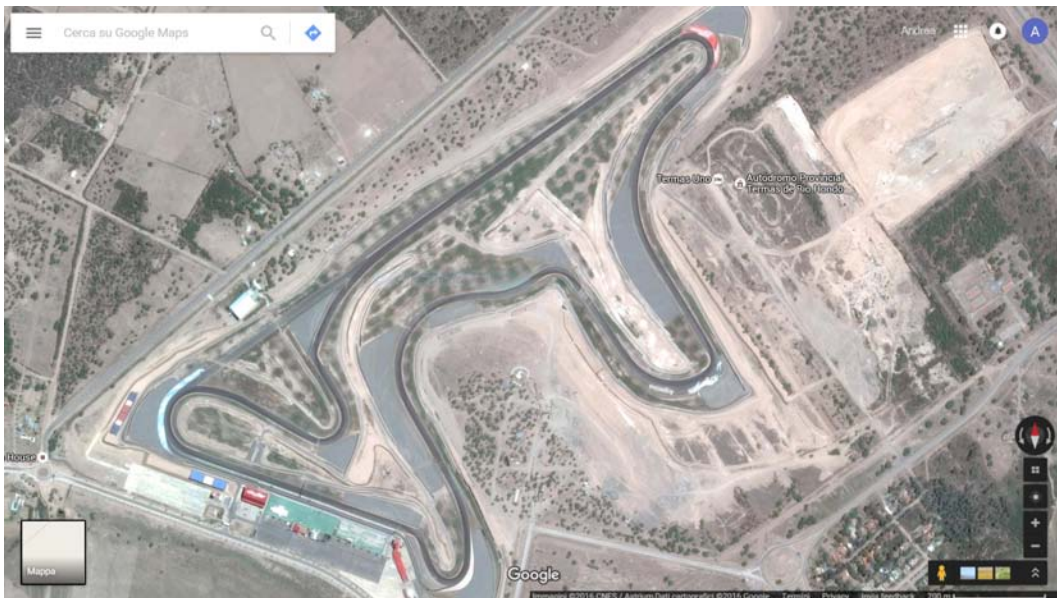


Figure 3.1: Argentina's track: view from Google Maps

The road ruby file required for XOptima is a sequence of arcs and lines, where the curves are defined by length and curvature while the straights simply by their length and zero curvature.

After that, we used a graphic software (*Rhinoceros*) to track the inner and outer edges of the circuit, but our interest is to the centreline. For this reason, we created four layer one for each part of the track and with the *CurveThroughPt* command we track the inner and outer edges. To rebuild the centreline we created a script with the *GrassHopper* tool. The input parameters required are the two curves just tracked (i.e. the inner and the outer edges), the direction of rotation clockwise or counter clockwise, the length and width of the track, and

other parameters. If all the required parameters have been entered correctly, you will see on the initial image, the centreline curve. Now, we have to redraw this line using the *polyline* command, making sure to use only arcs and line, tangents both incoming and outgoing. That done, we return of *GrassHopper* and always in input parameters, insert the line you just created in the centre polyline entry (see Fig.3.2).

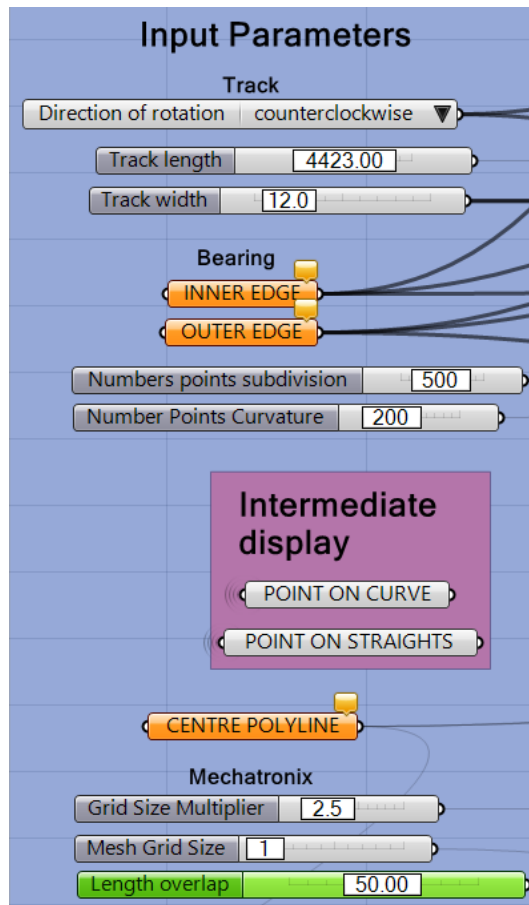


Figure 3.2: GrassHopper view: input parameters

If the centreline is designed properly, it will automatically generate the ruby files needed for optimal operation otherwise the file will be generated, but if a simulation was made, the track will be displayed incorrectly, remaining open. As seen in the Figure 3.3, the file is composed of several segments where it is reported length and curvature, if the curvature is zero means that the stretch is straight while for the various parts of a curve shows the curvature. To save the file as Ruby, just double-click on the output of *grasshopper* file, copy and paste on notepad and save with .rb extension. The track will now



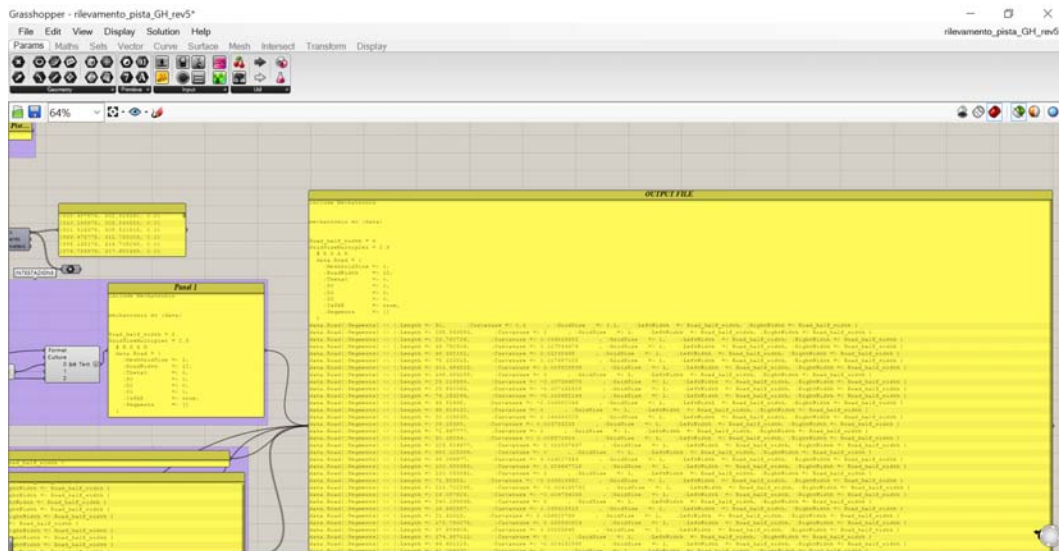


Figure 3.3: GrassHopper view: input parameters

loaded in *XOptima* files, so you have to change the OCP file so that it loads the track of our interest.

In Figure 3.4 the correct reconstruction of Termas de Río Hondo circuit, after simulating the track.

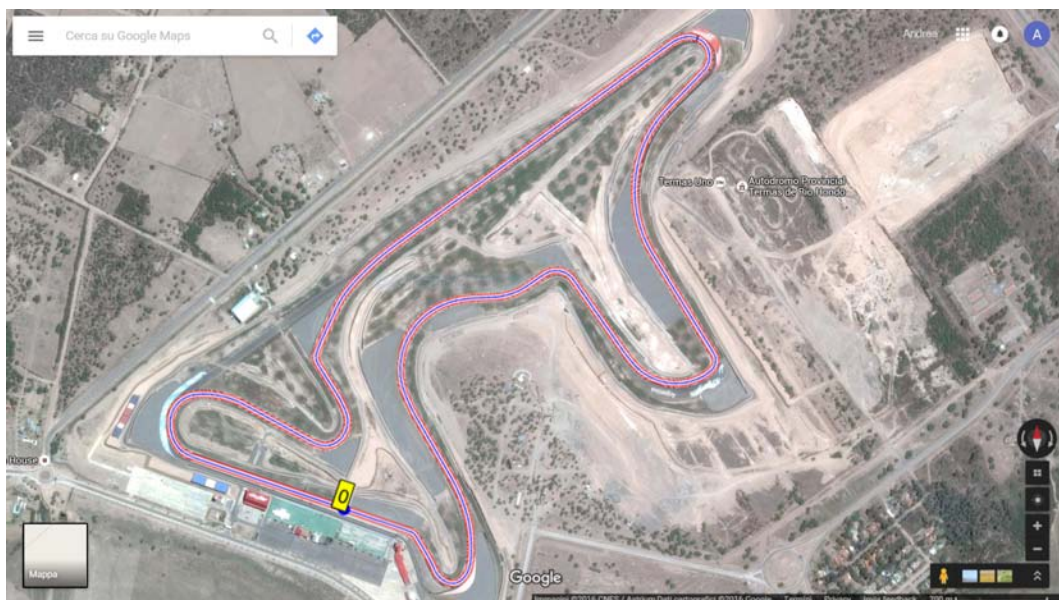


Figure 3.4: Reconstruction of Termas de Río Hondo circuit



# Chapter 4

---

## Model Validation

In this chapter we will discuss on how the model was validated. To give more strength to the theoretical basic and results of the optimal maneuver method, comparisons with data provided from telemetry of a Moto3 logged on 14-Nov-2015 at Valencia's track.

The vehicle model has been populated with the following data:

- mass, center of mass and inertia of the whole vehicle (measured);
- tyres (lateral characteristics measured, longitudinal estimated);
- rider (inertia estimated from weight and height);
- mass, center of mass and inertia of the front frame, front unsprung and swingarm (mass provided, inertia estimated);
- suspensions (provided);
- aerodynamic data (min drag provided, max drag estimated);
- engine torque (provided);
- gearbox and final transmission (provided);
- steering damper (estimated).

It is worth noting that the max friction coefficients of tyres have been set to 1.0 and 1.3 for longitudinal and lateral forces respectively. Such values may change depending on track conditions. The engine characteristic was modelled with a spline curve fitting nominal torque data as function of rpm. Below the simulation results in terms of trajectory, velocity, accelerations and roll angle are reported.

## 4.1 Comparison between Simulation and Telemetry

The simulation given by XOptima results in terms of velocity, torque and gear used are reported. The gearbox configuration is BEEEEB: primary 60/23 - first 31/16 - second 28/17 - third 23/16 - fourth 24/19 - fifth 28/25 - sixth 24/24. The simulation gearbox configuration is the same of the telemetry one.

The simulated minimum lap time with this configuration is 99.7s.  
The telemetry lap time with this configuration is 100.8s.

### 4.1.1 Velocity comparison: Telemetry vs. Simulation

A first comparison between the simulated speed and the telemetry one is represented in Figure 4.1

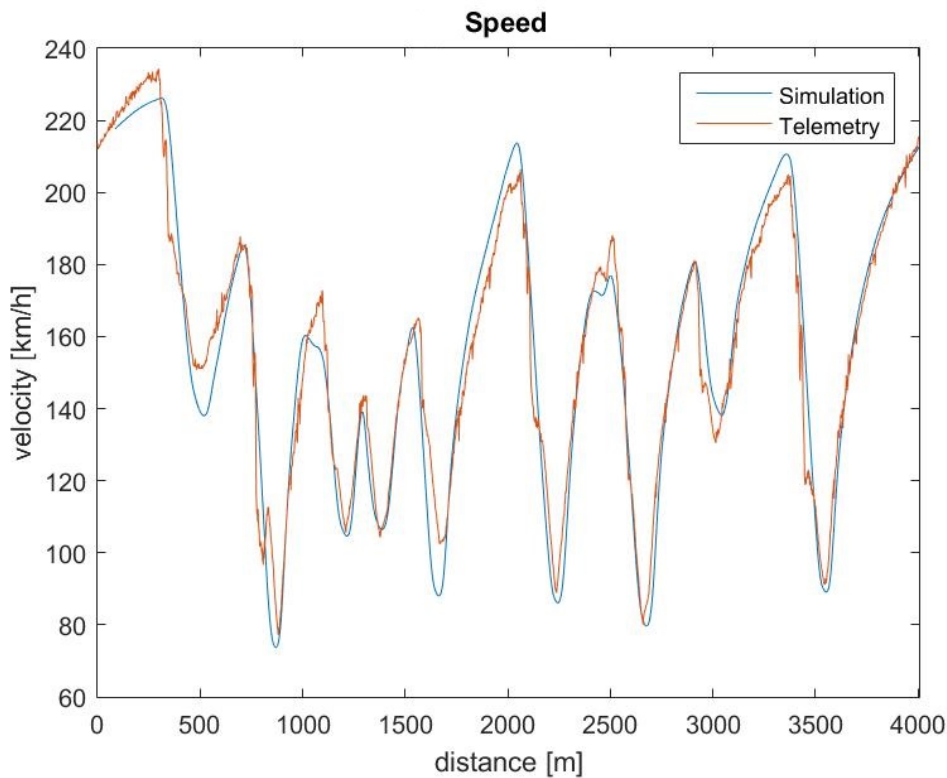


Figure 4.1: Velocity: Telemetry vs. Simulation correct

The telemetry forward speed does not consider the effect of tire toroidal radius

when the motorcycle is rolled (at a roll angle of 57 deg the rolling radius differs from the nominal radius by approx 8%).

In Figure 4.1 the simulation speed was adjusted in order to be compared with the telemetry, i.e. rear wheel spin rate times constant radius. The slope of the climb and descent fronts of the speed was taken as a reference to calibrate the xoptima parameters.

### 4.1.2 Gear shifting comparison: Telemetry vs. Simulation

In this section, we focus on the gear shifting. Figure 4.2 shows the comparison between telemetry and simulation. There are eight points with different gear shifting. The XOptima simulation does not consider the engine brake, so the simulated gear ratio in braking is not relevant in such condition. However, when the rider is using throttle, the use of a different gear can affect the maximum torque available. This will be addressed in the chapter 5.

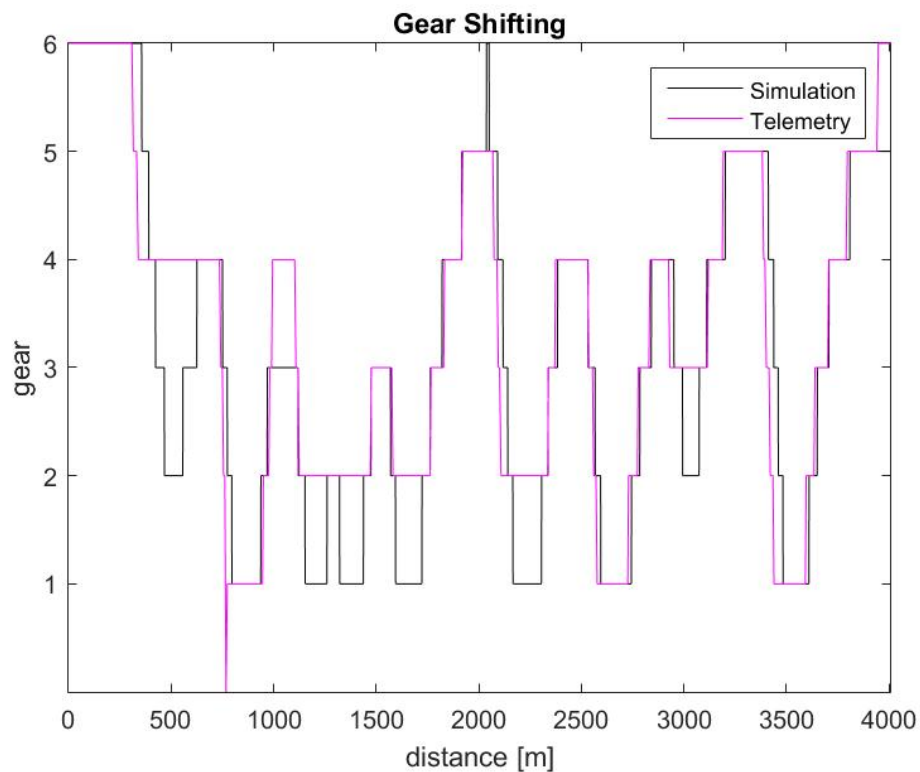


Figure 4.2: Gear Shifting: Telemetry vs. Simulation

### 4.1.3 Roll angle comparison: Telemetry vs. Simulation

Another compared parameter is the roll angle as shown in Figure 4.3.

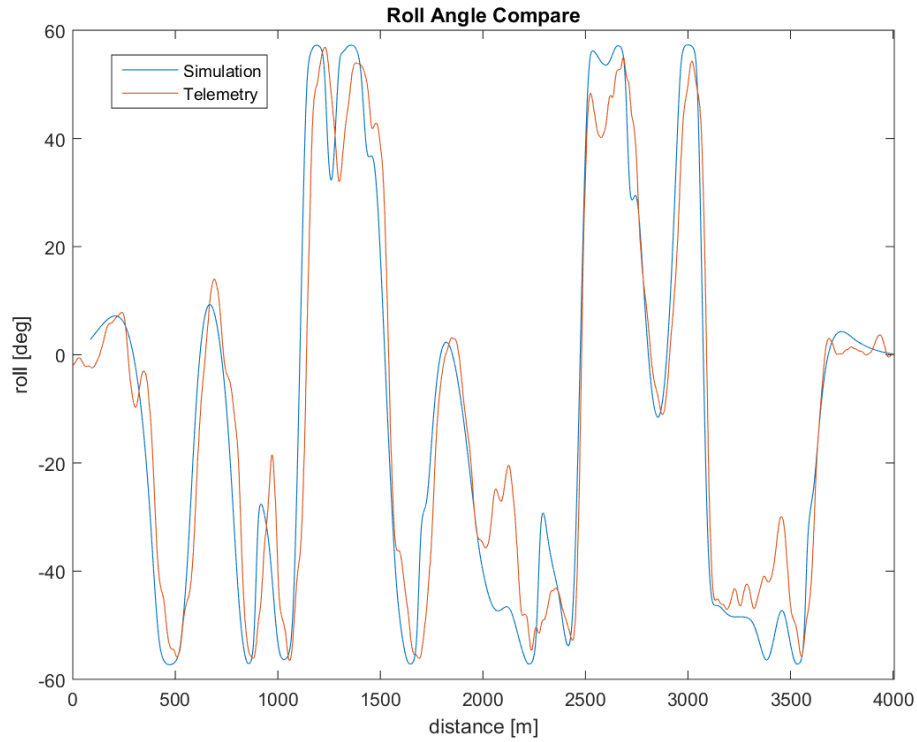


Figure 4.3: Roll angle: Telemetry vs. Simulation

This has less importance than the other, because for an accurate analysis is required the position of the motorcycle on track, that is not reported in telemetry supplied.







# Chapter 5

## Analysis of a Racing Motorcycle

After having properly calibrated the software as indicated on the chapter 4 we switched to analyse the results. Firstly, we considered to use the Optimal Maneuver Method to adjust the gearbox ratios in order to obtain improved performance, i.e. reduce lap-time. The gearbox ratios to be modified are the ones of the telemetry, and next will be referred as reference configuration. The analysis is carried out only on theoretical basis, without experimental tests of the new set of gearbox ratios. However, the simulated results are expected to be reliable, having previously calibrated the tool. According with the discussion above, new sets of gearbox ratios were tested on the same circuit. We tested all combinations, based on available gearwheel, which includes two solutions for each gear and two solutions for the primary ratios.

Gearing set								
Gear	Plan.	Ratio	Gear	Plan.	Ratio	Gear	Plan.	Ratio
1 <sup>st</sup>	A	30/16	2 <sup>nd</sup>	A	29/18	3 <sup>rd</sup>	A	28/20
	B	31/16		E	28/17		E	23/16
Gear	Plan.	Ratio	Gear	Plan.	Ratio	Gear	Plan.	Ratio
4 <sup>th</sup>	A	26/21	5 <sup>th</sup>	A	22/20	6 <sup>th</sup>	A	26/27
	E	24/19		E	28/25		B	24/24

Primary Ratio		
Gear	Plan.	Ratio
Primary	A	62/21
	B	63/21

More than 128 combinations were taken into considerations, but **no one** has led to a significant result.

## 5.1 Gear shifting analysis

As we discussed in the previous chapter we will now analyse the differences of the gear shifting between the result of simulation and the telemetry. Take back the Figure 4.2, reported in chapter 4, and revived below:

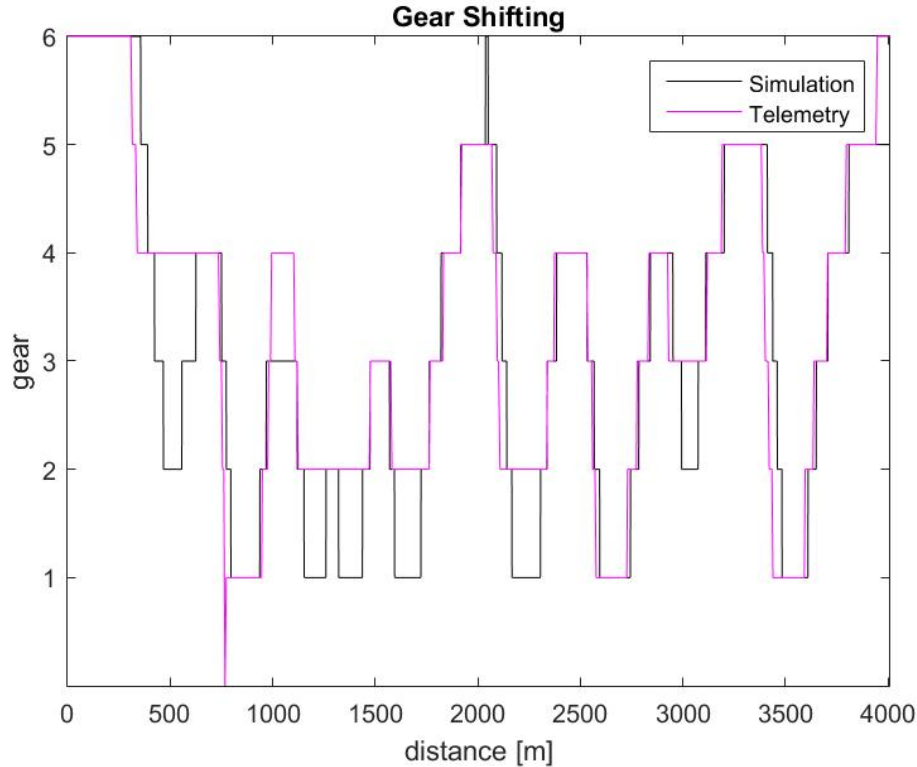


Figure 5.1: Gear Shifting: Telemetry vs. Simulation

In order to understand if the utilisation of a different gear by the real driver can affect the minimum time, Figure 5.2 shows the torque used by the simulation and the maximum torque available both with the gear engaged by the simulation and with the gear engaged by the real driver. The number of the turns, are shown within yellow boxes in Figure 5.2 and in Figure 5.3.

Analysing Figure 5.2, we can see that when exiting the curves 3, 4 and 5 the torque used by the simulation is below the maximum torque available with gear engaged by the real driver, therefore using a gear instead of another is irrelevant from the simulation point of view. On the contrary some important considerations can be made for the curves 1, 6, 8 and 12:

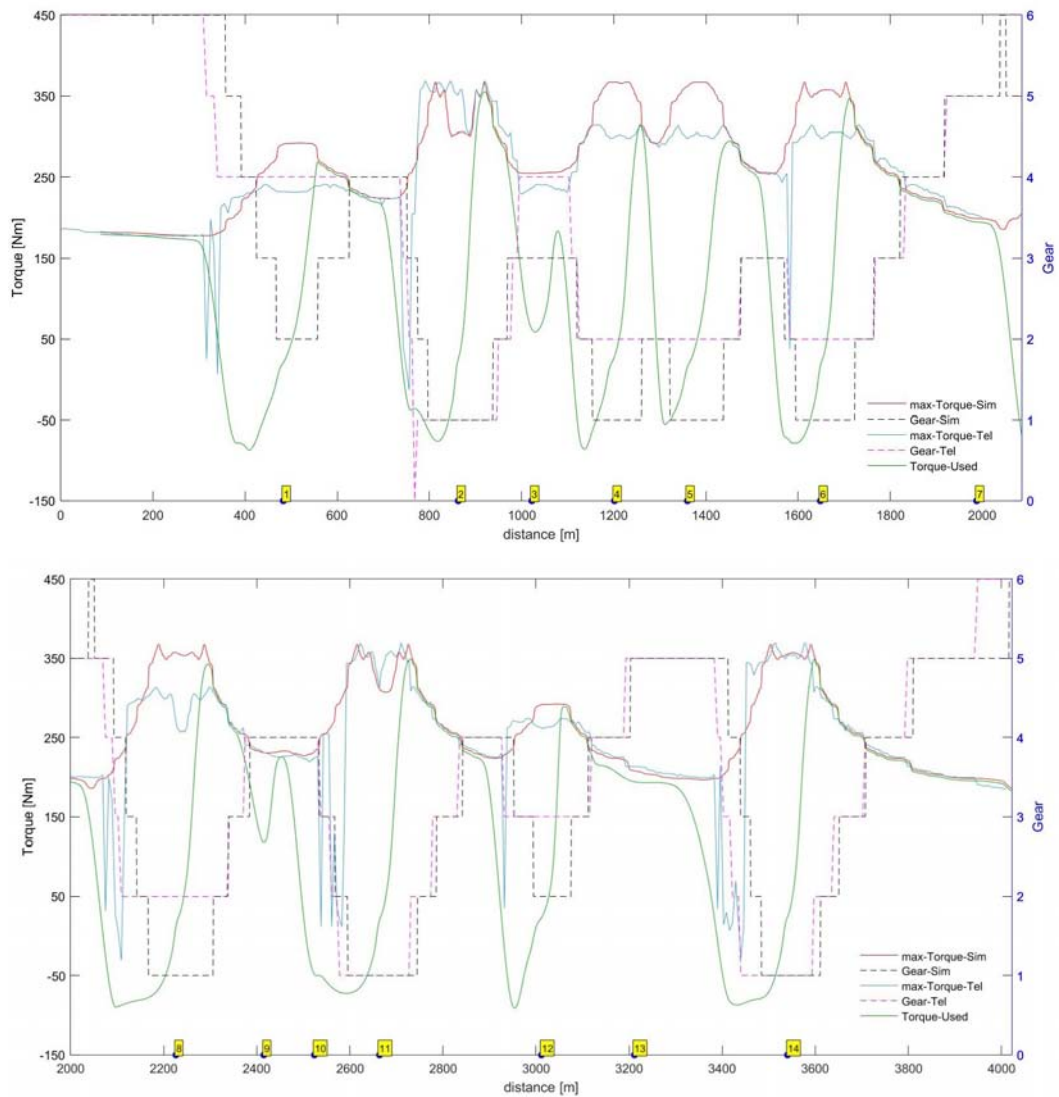


Figure 5.2: Gear Shifting and Torque max: Telemetry vs. Simulation

- In curve 1, when accelerating out of the turn, the torque-used by the simulation is above the maximum available torque used by the real driver. This happens for a time equal to 1.85s, which corresponds to a distance of 77m.
- In curve 6 the torque-used on simulation is above the maximum available torque for a time equal to 1.03s, which corresponds to a distance of 31m.

- In curve 8 the torque-used on simulation is above the maximum available torque for a time equal to 1.44s, which corresponds to a distance of 45m.
- In curve 12 the torque-used on simulation is above the maximum available torque for a time equal to 0.59s, which corresponds to a distance of 23m.

For the curve 7 it would not be feasible for the real driver to shift up and down in 0.25s as the simulation does. Summarizing, the use of a different gear while exiting curves 1 (downshift to 3<sup>rd</sup> instead of 4<sup>th</sup>) and 8 (downshift to 2<sup>nd</sup> instead of 3<sup>rd</sup>) may give some advantage on the lap time because more torque would be available for 1.4-1.8s. The driver may not be able to insert the correct gear for other reasons which may be a physical limit as the roll angle or for dynamic reasons as the engine brake.

Figure 5.3 shows the numbering of the curves in the Valencia's track. This numbering has been taken as a reference also to the earlier figures.

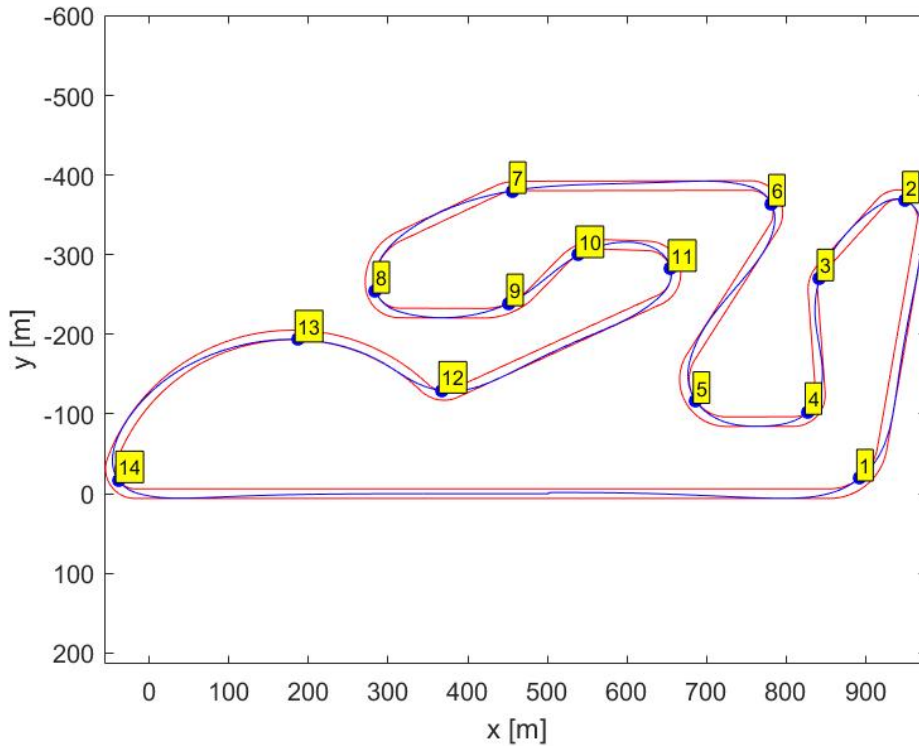


Figure 5.3: Trajectory with curves index

## 5.2 New throttle body analysis

It was possible to analyse the behaviour of the motorcycle with a new throttle body. The latter has been developed with the intent to provide a better exploitable torque curve. Simulations are performed in Valencia's track, with the same configuration used for the previous sections.

### 5.2.1 New throttle body vs old throttle body

Figure 5.4 shows the maximum torque available at wheel hub versus the bike speed, with the assumption of a constant wheel radius of 298mm. Different colours refer to different gears.

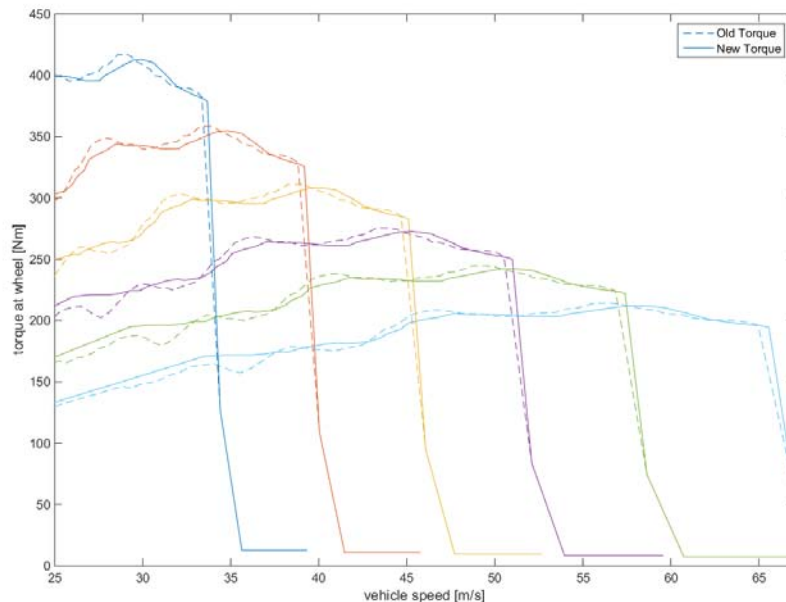


Figure 5.4: Torque provide by new and old throttle body

The lap time resulting from the simulation is of 99.631s (1:39:631), which is 0.05s faster than lap time obtained with the old throttle body. Fig.5.5 shows the speed of the motorbike, together with the speed difference (new throttle body speed minus old throttle body speed).

It can be observed that the new throttle body allows the motorbike to be faster in all straights. The short transients where it results to be slower is due to different braking/traction maneuvers, and they do not cause any performance loss.

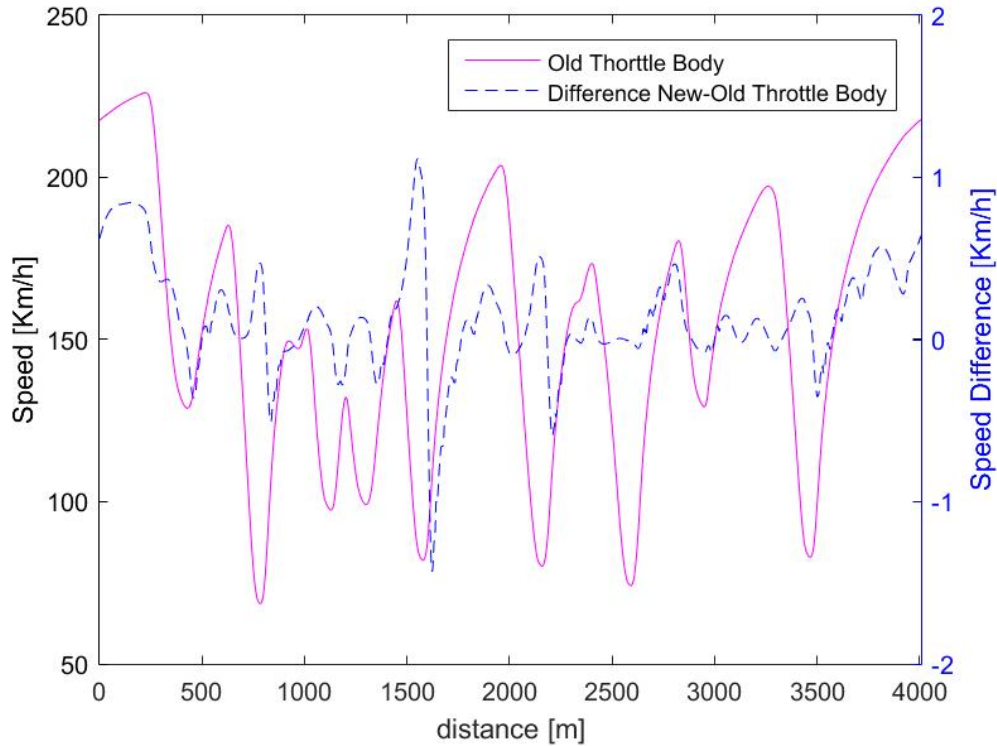


Figure 5.5: Different speed between new and old throttle body

As in the previous section highlighted that in some turns the driver was not able to exploit all engine power because he was using a too high gear; this was demonstrated to happen in turns 1,6,8 and 12. Thus, we are going to analyse if the new throttle body can bring any advantage in such situations. Fig.5.6 shows the engine torque used by the ideal driver, together with the maximum torque available with the gear engaged by the real driver (both with the old and new throttle body).

Fig.5.6 highlights that, even if the new throttle body provide a better overall performance, it decreases the available torque in the turns where the driver is engaging an higher gear and he complains about lack of traction. Indeed, in turns 1,6,8 and 12, the torque provided by the old throttle body with the gear engaged by the driver is higher than that provided by the new one. Looking back at Fig.5.4 , it can be noticed that whenever the driver would use an higher gear, the new engine results to be less perform powerful.

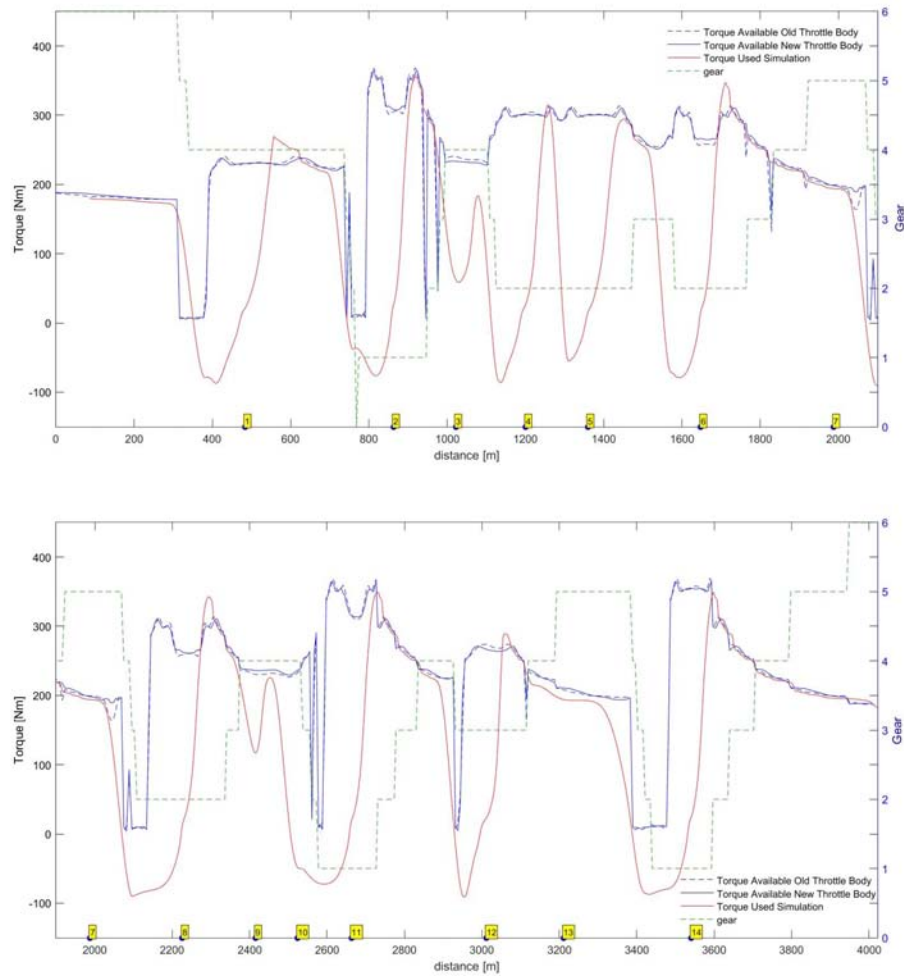


Figure 5.6: Different maximum torque between new and old throttle body

### 5.2.2 Considerations

On the basis of the simulation outcomes, we can state that the new throttle body allows the driver to be faster in those turns where he is able to engage the correct gear (i.e. the gear that provide the highest torque). However, whenever he is forced to engage an higher gear due to handling necessities, the new throttle body can exacerbate the lack of traction.

At the points where the driver does not engage the same gear determined from XOptima, can not to ground all the available torque, wasting time and traction. It must also be said, as for the previous section (5.1), it is not said that the driver unable to insert the correct gear for other reasons which may

be a physical limit (as the roll angle) or for dynamic reasons (as the engine brake), that the XOptima model disregards.

### 5.3 New gearing set analysis

In this section we analyse the new gearing set that has been proposed for 2016 season. Simulations are performed again in Valencia's track, with the same configuration used as reference in all the other cases.

All the simulations have been executed with both throttle body D and E (i.e. respectively, the old and the new throttle body)

The characteristics of the 2015 baseline and 2016 baseline gearing set that are going to be compared are reported in the following table:

Gearing set						
	2015			2016		
First	B	31/16	1.938	G	32/15	2.133
Second	A	29/18	1.611	D	31/17	1.824
Third	A	28/20	1.400	D	27/18	1.500
Fourth	A	26/21	1.238	B	26/20	1.300
Fifth	A	22/20	1.100	D	21/18	1.167
Sixth	B	24/24	1.000	F	19/18	1.056
Primary	62/21			61/23		
Wheel ring/pinion	38/16			39/17		

#### 5.3.1 Summary

The comparison of the vehicle speed as function of the engine rpm for the baseline 2015 (old) and baseline 2016 (new) gearing set is shown in Fig.5.7.

Fig.5.7 shows that the 2016 baseline provides on average a longer gearing set, and the difference between the two gearing set are most noticeable with the higher gears; indeed, the 5th gear of the 2016 is almost equal to the 6th of the 2015.



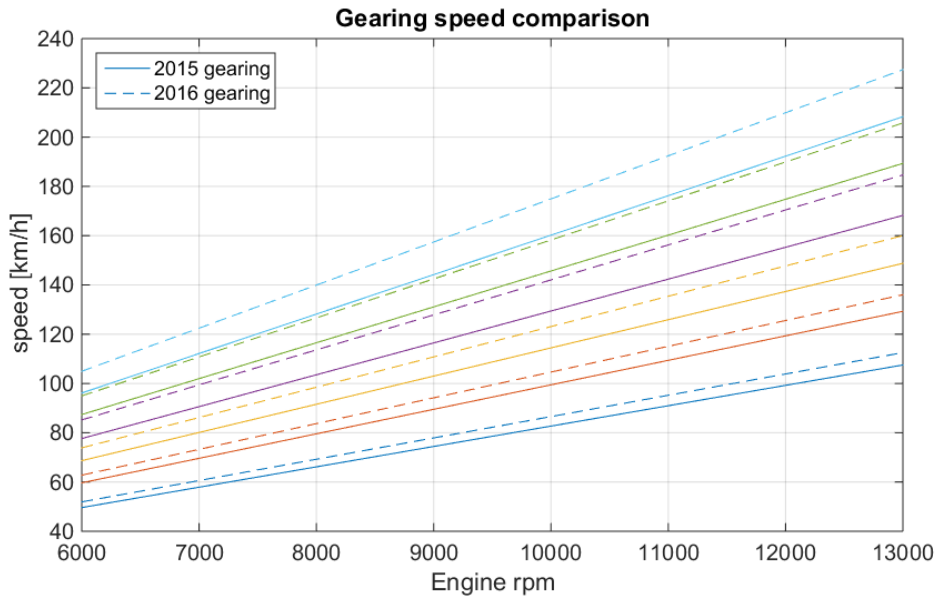


Figure 5.7: Motorbike speed vs engine rpm with the 2016 and 2015 gearing set

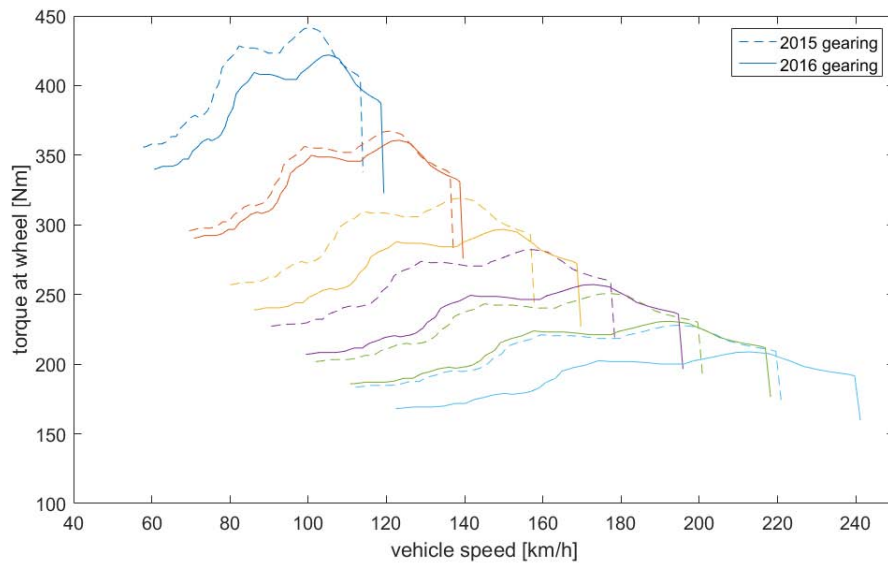


Figure 5.8: Torque at wheel envelope with throttle body E

Fig.5.8 torque at wheel envelope with throttle body E and Fig.5.9 torque at wheel envelope with throttle body D show the maximum torque available at the rear wheel for each gear, respectively with the throttle body E and D. Such

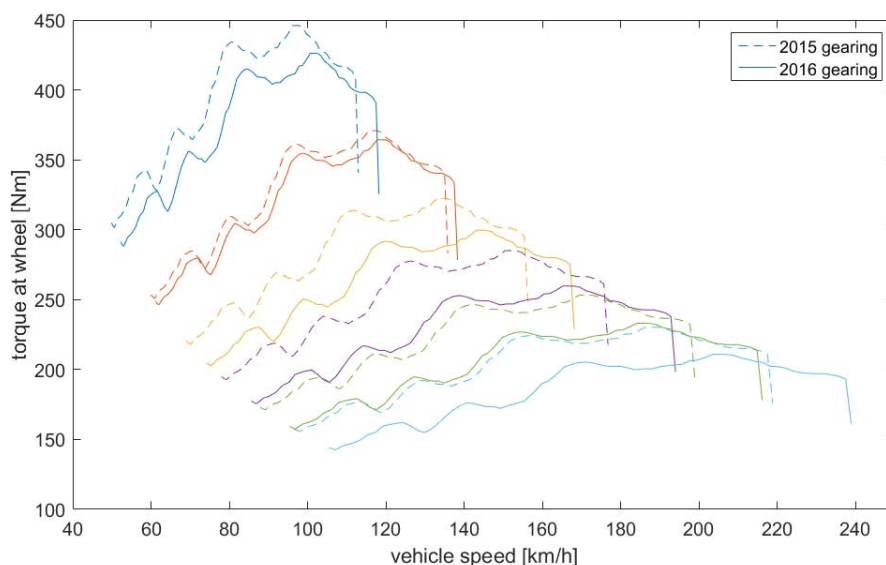


Figure 5.9: Torque at wheel envelope with throttle body D

figures highlight that with the 2015 gearing set in the gear shifts are generally closer; in particular, with the throttle body E (Fig.5.8), except for the first gear shift between 1st and 2nd gears, after all the other gear shifts the engine is working approximately at its torque peak rev rate. With the throttle body D (Fig.5.9) the behaviour is similar, but the gear shifts between 4<sup>th</sup>-5<sup>th</sup> and 5<sup>th</sup>-6<sup>th</sup> occur at a slightly higher engine rev rate. With both E and D throttle bodies, when the second gear is engaged the engine is at a rev rate significantly before its torque peak.

In the 2016 gearing set all the gears are generally longer, thus after each gear shift the engine is at a lower rev rate comparing the 2015 gearing set. Moreover, the 1st and 2<sup>nd</sup> gear appear to be closer, while between the 2<sup>nd</sup> and 3<sup>rd</sup> there is much more gap: indeed, when the 3<sup>rd</sup> gear is engaged, the engine is far before its maximum torque peak. The same happens when the 4<sup>th</sup> gear is engaged and the throttle body E is used.

The following table summarizes the best lap-time obtained for the 2015 and 2016 gearing set, with both throttle bodies D and E:

	<b>Gear 2015</b>	<b>Gear 2016</b>	<b>2016-2015</b>
	<b>Time [s]</b>	<b>Time [s]</b>	<b>difference Time [s]</b>
<b>Throttle body D</b>	99.748 s	99.731 s	-0.017 s
<b>Throttle body E</b>	99.671 s	99.692 s	0.021 s

The 2016 gearing set is approximately 0.02s faster than the 2015 one when the throttle body D is used, and it is slower nearly of the same amount when the throttle body E is used.

A more detailed analysis of the differences between the two gearing set will be performed in the next section.

### 5.3.2 Simulation results

The motorbike speed along Valencia track, together with the speed difference between 2016 and 2015 gearing set, is shown in Fig.5.10 and reports the simulated data with the throttle body E, while Fig.5.11 with the D one. Both Fig.5.10 and Fig.5.11 show that the 2016 gearing set allows to reach higher speeds in the main straight (2015 gearing seems too short as long as the engine hit its maximum rev rate with the 6<sup>th</sup> gear), while it is slightly slower in the accelerations out of the turns; this agrees with the fact that the new gearing set is longer than the 2015 one. Moreover, the motorbike speed in the middle of the turns is generally higher with the 2016 gearing set, and this is a consequence of the lap-time minimisation process: as long as the acceleration has decreased using the 2016 gearing set, the motorbike now behaves like a slightly less powerful motorbike (when exiting a turn), and it is known that this lead to higher speeds at the middle of the turns. It can be noticed also that with the throttle body D the differences are significantly smaller, moreover in the last turn (the 14<sup>th</sup>), the new gearing set allows to better accelerate out of such turn.

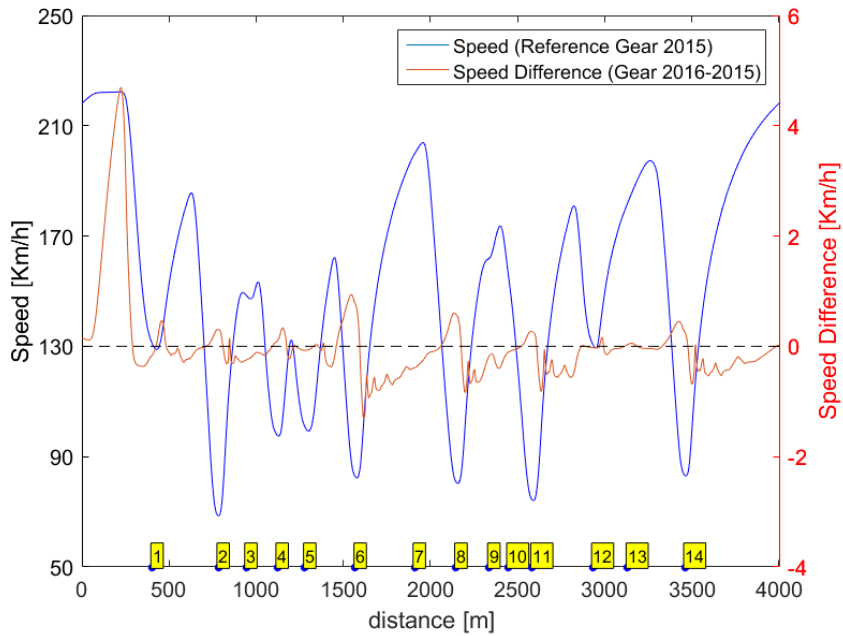


Figure 5.10: Speed profile and speed difference (throttle body E) - simulation

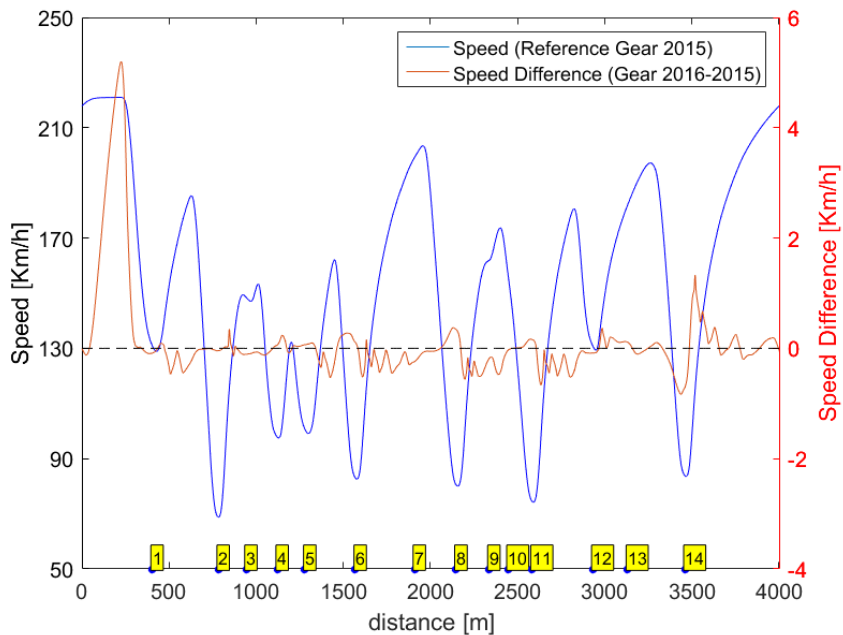


Figure 5.11: Speed profile and speed difference (throttle body D) - simulation

In the next figures we are going to analyse the maximum torque available in the fourth turns where the real driver experiences lack of traction. Fig.5.12 shows the maximum torque available with the gear engaged by the real driver (both with 2016 and 2015 gearing set), together with the torque used by the simulation. Fig.5.12 refers to the throttle body E, while Fig.5.13 to the D one.

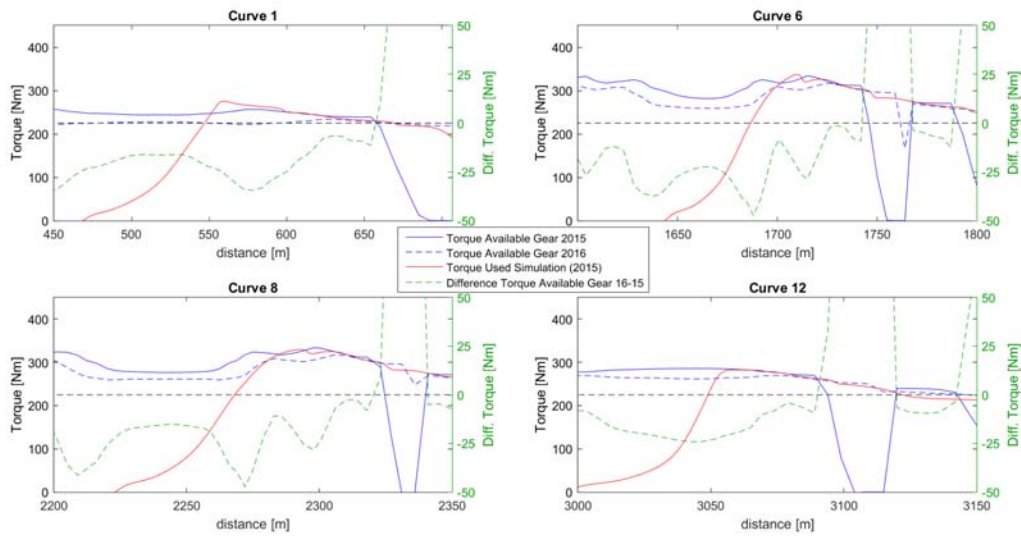


Figure 5.12: Torque available for the real driver and torque used by the simulation (throttle body E)

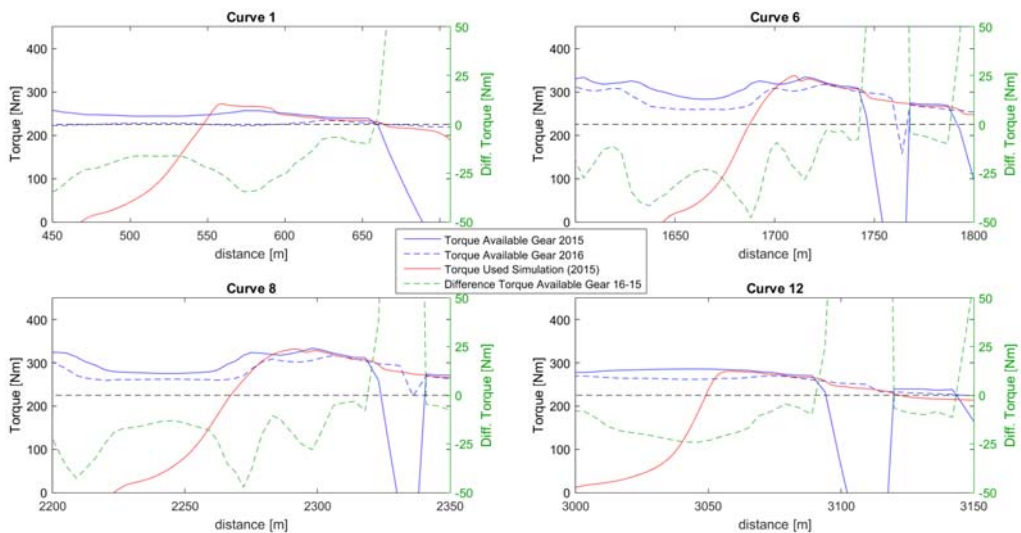


Figure 5.13: Torque available for the real driver and torque used by the simulation (throttle body D)

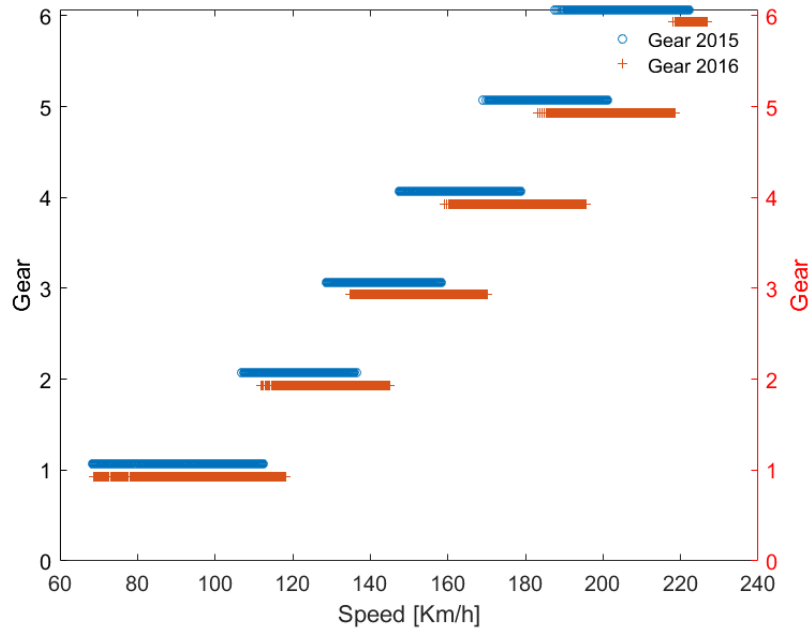


Figure 5.14: Engaged gear versus speed (throttle body E) - simulation

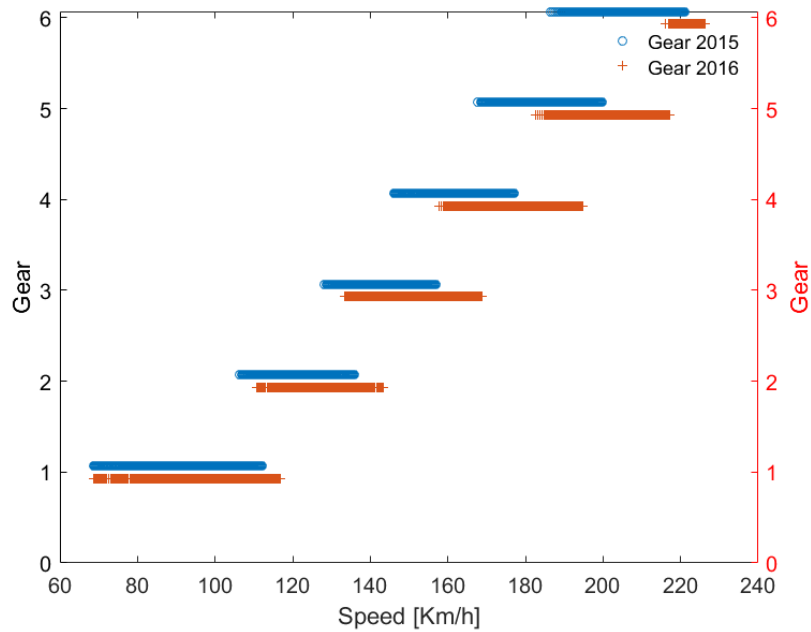


Figure 5.15: Engaged gear versus speed (throttle body D) - simulation)

Fig.5.14 and 5.15 show that with the 2016 gearing set the gear shifts occur at higher speeds. Moreover, it is evident that the 2016 gearing, in the configuration used in this simulation, seems too long for the Valencia track as long as the 6<sup>th</sup> gear is engaged for a small range of speeds. However, since the lap-time difference with the 2015 gearing is small, the 2016 gearing is very likely to give an advantage in real racing conditions where the driver is following another driver allowing to reach higher speeds.

### 5.3.3 Considerations

In this section the 2016 and 2015 baseline gearing set have been compared. From the analysis, it is evident that, with the sprocket-pinion configuration used, the 2016 gearing set is considerably longer than the 2015 one. In particular, the 2016 gearing set allows to reach higher speeds in the main straight even if no wake effect is exploited, suggesting that in real racing conditions it is more convenient than the 2015 one. Moreover, the 2016 gearing highlighted a noticeable greater shift gap between 2<sup>nd</sup> and 3<sup>rd</sup> gears.

In the turns 1, 6, 8 and 12, where the real driver experiences lack of traction, the 2016 gearing ratio diminishes the torque available to the driver (because it is a longer gearing). However, it might be possible that, being a longer gearing, the real driver could engage more easily a shorter gearing (i.e. a third instead of a fourth). Finally, the net lap-time difference between the old and new gearing set is only  $\pm 0.02s$ , being the 2016 faster or slower depending on the throttle body used, i.e. depending on the engine torque curve. Such limited theoretical lap-time difference suggests that human factors (i.e. the preference of the driver of a particular gearing in a certain turn) are very likely to overcome the real performance difference.





# Chapter 6

---

## Parametric analysis

We have seen in the chapter 5, optimizing gear and throttle body has not led to a significant reduction in lap time. The objective of this section is to use the Optimal Maneuver Method to improve the performance of a racing motorcycle changing other parameter different from those previously used (i.e. gearing set and throttle body). To do this we analyse how the sprocket-pignon ratio, the drag force, the inertia and the position of centre of mass influence the lap time. The analysis is carried out only on theoretical basis, without experimental tests.

### 6.1 Influence of the sprocket-pignon ratio

According to information derived from previous chapter a parametric analysis of sprocket-pignon was tested on the same circuit. The number of teeth of sprocket and the number of teeth of pignon have been changed as follows:

- N\_sprocket: 37:1:42
- N\_pignon: 15:1:19

The reference time 99.677s refers to the configuration with N\_sprocket=39 and N\_pignon=17. The variation of the sprocket ratio (i.e. the diameter) affects the squat. Consider the intersection point A, between the axis of the upper branch of the chain and the straight line passing through the center of the wheel and the swingarm pivot, shown in Figure 6.1. The straight line connecting the contact point between the rear wheel and the point A, is called *squat line*. Its inclination with respect to the horizontal plane is called *squat angle*  $\sigma$ .

The straight line of action of the resultant  $F_r$  is called *load transfer line*, and it is inclined at an angle  $\tau$ .

Is defined as the squat ratio  $\mathfrak{R}$ , the ratio of the moment generated by the load transfer and the moment generated by the sum of the squat force and the driving force:

$$\mathfrak{R} = \frac{\tan \tau}{\tan \sigma} \quad (6.1)$$

There are three cases:

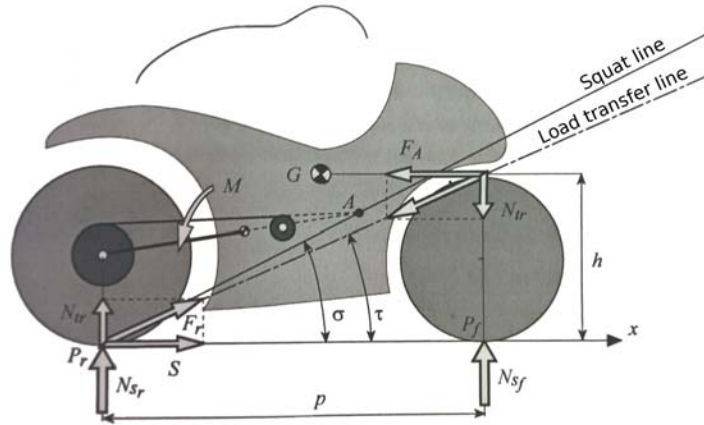


Figure 6.1: Squat and Load transfer lines

- the point A lies on the line of the load transfer or rather  $\sigma = \tau$ ; in this case  $\mathfrak{R} = 1$ . During the boost phase, there are no additional moments acting on the swing arm, so the suspension spring is no longer stressed with respect to the static position;
- the point A is located below the straight line of the load transfer, or rather  $\sigma < \tau$ ; in this case  $\mathfrak{R} > 1$ . The moment generated by the resultant, causes an additional compression of the spring in addition to the one created by the static load;
- the point A is located above the straight line of the load transfer, or rather  $\sigma > \tau$ ; in this case  $\mathfrak{R} < 1$ . The moment generated by the resultant causes an extension of the spring;

Change of diameters of sprocket and pinion corresponds to moving the point A, which results to one of the above situation. When mounting a larger sprocket, the wheel pivot approaches the centre of mass, which corresponds to a decrease of the wheelbase. The load on the rear wheel increases, improving the holding, but worsening the stability of the bike under braking. On the contrary, by mounting a smaller sprocket, the wheel pivot turns away from the centre of mass, which corresponds to an increase of the wheelbase. It causes a slight loss of traction for the decrease of the load on the rear wheel, instead, increasing the load on the front wheel. In this case, it improves braking stability, but a

greater difficulty turning through tight corners or in fast reverse.

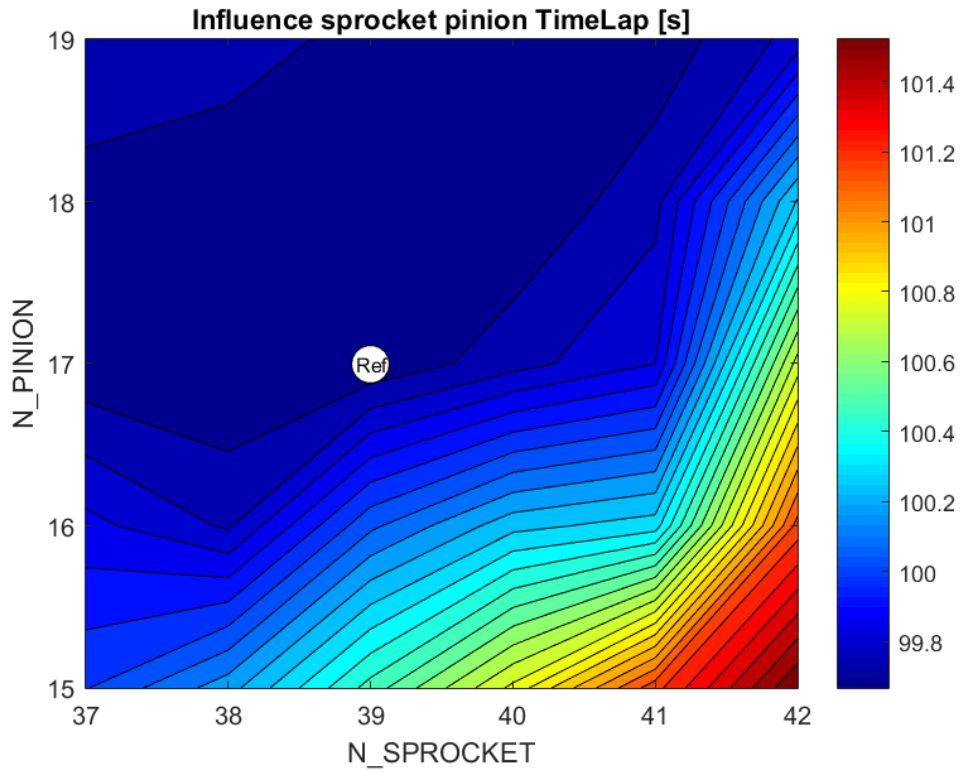


Figure 6.2: Map of the lap times due to the variation of sprocket pinion ratio.

Whereas a suspension as in Figure 6.1, we calculated the value of the squat ratio  $\mathfrak{R}$  with the values of sprocket and pinion indicated in Figure 6.2. In the reference configuration  $\mathfrak{R} = 0.90^\circ$ , in the case with the larger sprocket and the smallest pignon (42-15)  $\mathfrak{R} = 0.83^\circ$ , in the opposite case (i.e. larger pignon and the smallest sprocket, 37-19)  $\mathfrak{R} = 0.98^\circ$ . In all cases into account the squat ratio is less than one, but close enough.

We see in the Figure 6.2, there is not an optimum value which maximizes the performance but a range in which the lap time remains almost unchanged. In agreement with what was said before, increasing too much the number of teeth of the stocker with a small pinion, lap time rises, probably to excessive skidding of the rear wheel.

## 6.2 Influence of the centre of mass position

In order to perform an optimization of the position of the centre of mass of the vehicle, a parametric analysis has been carried out. The choice of this parameter is due to its paramount importance and to the possibility of adjusting it in real races.

The height  $h$  and the lateral position  $b$  of the centre of mass have been changed as follows:

- $h$ : 0.448:0.01:0.488
- $b$ : 0.643:0.01:0.683

The reference time 99.677s refers to the configuration with  $b=0.663$  and  $h=0.468$ . With respect to acceleration, have shown in [9], the limit between the two possible behaviour of a motorcycle: the wheeling and the skidding of the rear tire, is mostly due to the longitudinal adherence tire coefficient and to the ratio  $b/h$ , between the longitudinal and the vertical position of the centre of mass.

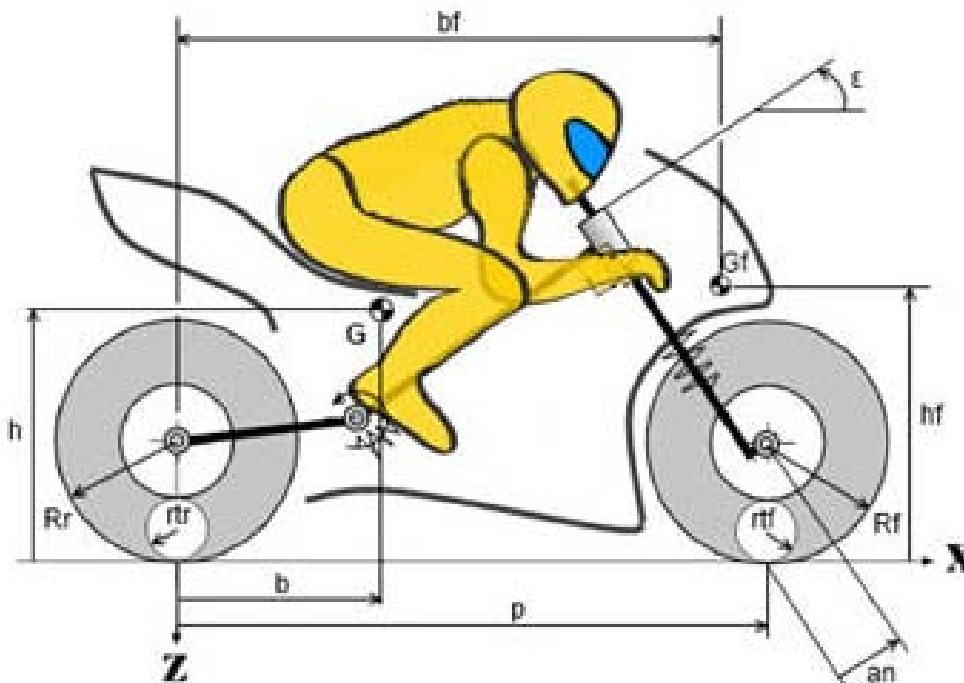


Figure 6.3: Model of racing motorcycle.

It is important to notice that, if a motorcycle is not powerful enough the wheeling can not spontaneously occur. The limit of the acceleration for wheeling is given by:

$$\ddot{x} = g * \frac{b}{h} \quad (6.2)$$

where  $g$  is the gravity acceleration. That is  $14.95m/s^2$  for the reference position of the centre of mass and corresponds on  $2098N$  of longitudinal force that is more than the engine can provide. Furthermore, if the worst situation for wheeling is considered (lowest  $b$  and highest  $h$ ), the limit for acceleration is  $12.93m/s^2$  that corresponds on  $1814N$  of longitudinal force that is once again more than the engine's possibilities.

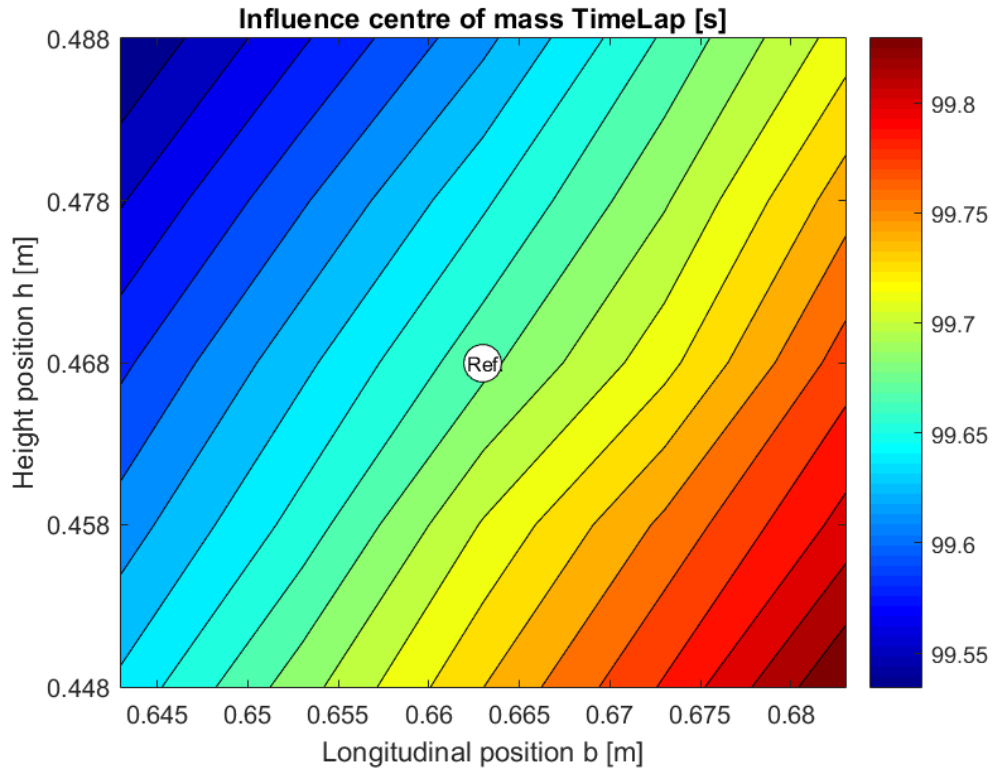


Figure 6.4: Map of the lap times due to the variation of the position of the centre of mass.

According with Figure 6.4, the movement of the centre of mass upward and

backward allows higher load transfers from the front wheel to the rear one and higher static loads on the rear wheel improving traction, without any problems of wheeling. An important observation is that, the height and the longitudinal position of the centre of mass have about the same weight in order to reach the settings of minimum lap time.

### 6.3 Influence of Roll and Yaw inertia

The objective of this section is to analyse whether the inertia along the x-axis (Roll) and z-axis (Yaw) influence lap time, through parametric analysis. Inertias were varied as follows:

- I<sub>x</sub> (Roll inertia): variations of 5%, 10%, 25%;
- I<sub>z</sub> (Yaw inertia): variations of 5%, 10%, 25%;

There were no significant changes to the lap time, nevertheless the trend which it was found is to increase roll inertia and decrease yaw inertia. For this reason, we have launched a new simulation doubling I<sub>x</sub> and halving I<sub>z</sub> obtaining an improvement on lap time of one cent (irrelevant).

### 6.4 Influence of the aerodynamic drag

The last parameter that we analyse is the influence of aerodynamic drag. As it has been mentioned in chapter 4, the drag coefficient on fairing is provided, while that during braking phase is estimated.

During acceleration the driver remains on fairing to decrease the air resistance, while during the braking phase, the driver gets up from the fairing increasing the frontal area and therefore increasing the drag force, as shown in Figure 6.5.

The drag force has been calculated as following:

$$F_{Drag} = \frac{1}{2} \rho * C_{DAA} * v^2 \quad (6.3)$$

$$F_{Drag} = \frac{1}{2} \rho * C_{DDA} * v^2 \quad (6.4)$$

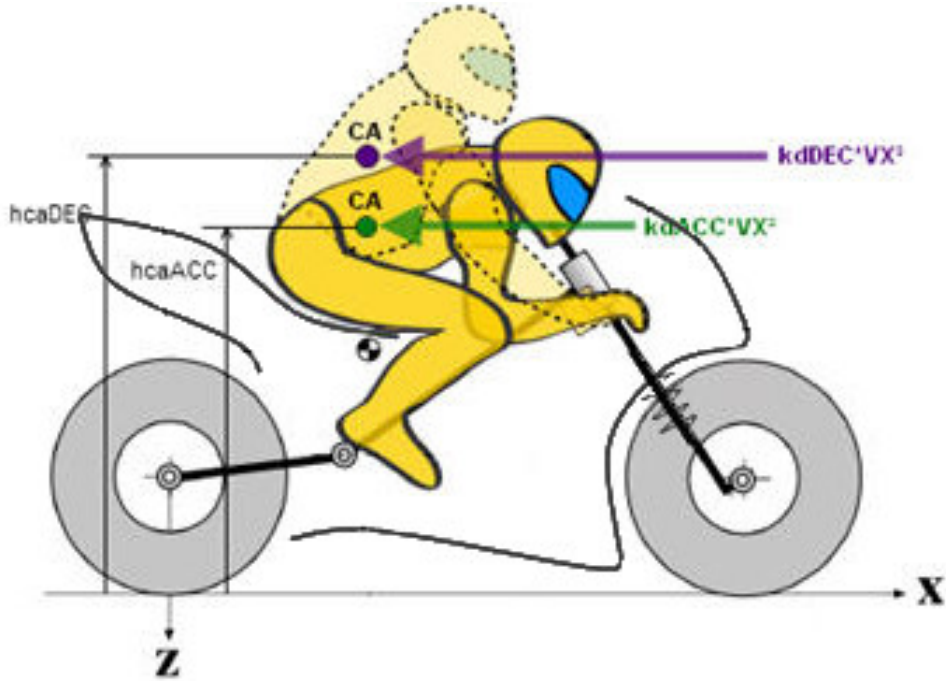


Figure 6.5: Model of drag, during acceleration and braking phase.

where  $\rho$  is the air density in  $kg/m^3$ ,  $C_{DA}$  is the drag coefficient during acceleration while  $C_{DD}$  is the drag coefficient during braking,  $A$  is the frontal area in  $m^2$  and  $v$  is the velocity of the motorcycle in  $m/s$ . More than the single drag coefficient we considered the set coefficient and frontal area  $C_D A$ .

The drag coefficient multiplied by the area during acceleration  $C_D A A$  and the drag coefficient multiplied by the area during braking  $C_D A D$  have been changed as follows:

- $C_D A A$ : 0.191:0.01:0.221
- $C_D A D$ : 0.4:0.025:0.5

which corresponds approximately to a variation of the the entire parameter of  $\pm 5\%$  and  $\pm 10\%$ .

The reference time 99.677s refers to the configuration with  $C_D A A = 0.201$  and  $C_D A D = 0.45$ .

In agreement with what we expected, the trend is to decrease the drag coefficient (or the frontal area) during the acceleration phase, while increase that during the deceleration phase, according with Figure 6.6.

Another important consideration, observing the Figure 6.6, is the inclination

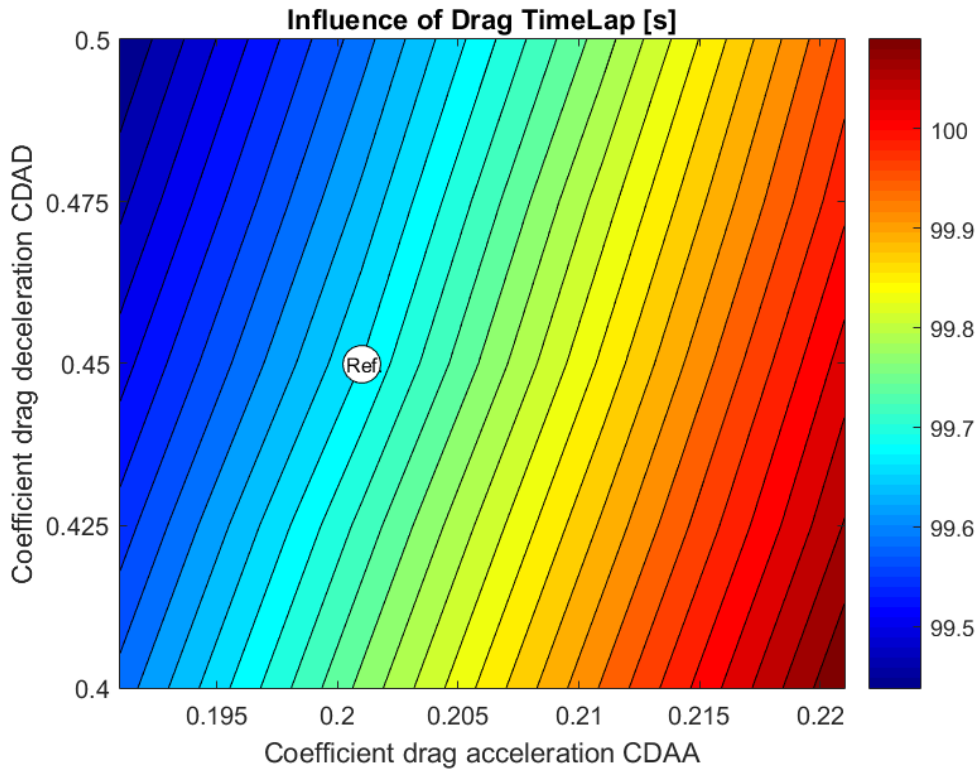


Figure 6.6: Map of the lap times due to the variation of the drag parameters.

of the straight lines. As you can see, with the same percentage variations of both parameters, the drag during acceleration is more influential than the drag during deceleration. This is because the driver spends more time on fairing during the entire circuit. It is not so uncommon to change the fairings to improve by a few percentage points of the drag values.







# Conclusions

In this thesis the optimal maneuver method has been applied to a racing motorcycle in order to minimize the time lap. The method produces realistic racing maneuvers as shown by the comparisons with data acquired on board of sports motorcycles. The comparisons with the experimental data show good agreement and suggest employing the method also to improve driver's skills and performance. For these reasons, it can be used to choose motorcycle parameters at the design stage and/or during motorcycle set up. In this work it was employed, firstly, to set up the gearbox to optimize the lap time in the Valencia's track and then to propose other solutions, in order to improve the lap time. The gearbox analysis was carried out with theoretical basis, simulation and comparisons with telemetry. Gear shifting analyses showed that the use of a gear lower than the one used by the driver while exiting some curves (reported in Section 5.1) may give some advantage on the lap time (some tenths of a second) because more torque would be available. The driver may not be able to engage the correct gear for the dynamics surrounding. For this reason, it would be interesting - as a future development - a more accurate model of the gearbox which takes account of the shifting times and the impossibility of shifting according to what is angled the motorcycle.

The throttle body analyses showed that the new throttle body allows the motorcycle to be faster in all straights, with an improvement in lap time of 0.05 s. Even if the new throttle body provides a slightly overall performance, it decreases the available torque in the turns where the driver engages a higher gear and the new throttle body results to be less powerful in terms of exiting traction of the said curves.

When comparing the two gearing set analysis, it is evident that, with the sprocket-pinion configuration used, the new gearing set is considerably longer than the old one. In particular, the new gearing set allows to reach higher speeds in the main straight even if no wake effect is exploited. The new gearing ratio also diminishes the torque available to the driver (because it is a longer gearing) and it might be possible that the real driver can more easily downshift. Finally, the net lap-time difference between the old and new gearing set is only  $\pm 0.02s$ , being the new faster or slower depending on the throttle body used, i.e. depending on the engine torque curve.

All the gearbox analyses showed that there is a change of net benefit and the human factors, not considered in the simulated model, are determined for the real difference lap.

More significant is the parametric analysis where we saw the influence of the sprocket-pinion ratio, the centre of mass position, the inertia and the drag.

As regards the influence of the sprocket-pignon, there is a bound where the lap time remains almost unchanged, the time lap difference between the best and the worst configuration is about 2 seconds.

The influence of the centre of mass position, shows that there is an optimum configuration which minimizes the time lap. In this case the time lap difference between the best and the worst configuration is about 0.3 seconds.

As we saw in section 6.3, the inertia does not affect the time lap appreciably. Finally, the influence of the drag, shows (like as the position of the centre of mass) that there is an optimum configuration which minimizes the time lap. In this case the time lap difference between the best and the worst configuration is about 0.5 seconds.

Additional mathematical models can be developed to address the limitations of current models.





# Bibliography

- [1] V.Cossalter, M.Da Lio, R.Lot and L.Fabbri, "*A general method for the evaluation of vehicle manoeuvrability whit special emphasis on motor-cycles*", Vehicle System Dynamics, vol. 31, no.2, pp. 113-135, 1999.
- [2] M. Da Lio, "*Analisi della manovrabilità dei veicoli. Un approccio basato sul controllo ottimo*", ATA Giornale dell'Associazione Tecnica dell'automobile, 50-1, pp.35-42,1997.
- [3] V.Cossalter, M.Da Lio,F.Biral, L.Fabbri,"*Evaluation of Motorcycle Manoeuvrability with the Optimal Manoeuvre Method*", SAE Meeting, 1998 Motorsports Engineering Conference&Expositon, Dearborn, Michigan, 16-19 november 1998 - SAE Transaction - Journal of Engines, 1998.
- [4] E.Bertolazzi, F.Biral, M.Da Lio and V.Cossalter, "*The influence of rider's upper body motion on motorcycle minimum time maneuvering*", in Multibody Dynamics 2007, ECCOMAS Thematic Conference, Milan, Italy, June 2007.
- [5] V.Cossalter, S.Bobbo, M.Massaro and M.Peretto, "*Application of the optimal maneuver method for enhancing racing motorcycle performance*", SAE International Journal of Passenger Cars - Electronic and Electrical System, vol.1,no.1,pp. 1311- 1318,2009.
- [6] F.Biral,R.Lot,M.Peretto, "*Optimization of the Layout of a Racing Motorcycle using the Optimal Maneuver Method*", IAVSD 2007.
- [7] F. Biral, M. Da Lio, F. Maggio,"*How Gearbox Ratios Influence Lap Time and Driving Style. An Analysis Based on Time-Optimal Maneuvers*", SAE Paper 2003-32-0056 / 20034356.
- [8] V.Cossalter, R.Lot, D.Tavernini, "*Optimization of the centre of mass position of a racing motorcycle in dry and wet track by means of the Optimal Maneuver Method*",Mechatronics (ICM), 2013 IEEE International Conference, pp. 412-417.
- [9] V.Cossalter, *Motorcycle Dynamics*, Lulu.com, Raleigh, North Carolina, 2006.
- [10] S.M.Savaresi, D.Ciotti, M.Sofia, E.Rosignoli and E.Bina, "*Gear-set optimization of a race car*", 2006 IFAC, pp. 579-584.

- [11] S.M.Savaresi, C.Spelta, D.Ciotti, M.Sofia, E.Rosignoli and E.Bina, "*Virtual selection of the optimal gear-set in a race car*", International Journal Vehicle System Modelling and Testing, Vol.3, Nos.1/2, 2008, pp. 47-67.
- [12] P.Giani, F.Todeschini, M.Tanelli, S.M.Savaresi and M.Santucci, "*Automatic Gear Shifting in Sport Motorcycles*", IEEE Transactions on vehicular technology, Vol.36, No.5, June 2014.
- [13] M.Pettersson and L.Nielsen, "*Gear Shifting by Engine Control*", IEEE Transactions on control system technology, Vol.8, No.3, May 2000.
- [14] D.Tavernini, "*Sport vehicles and virtual riders modeling*", PhD thesis, University of Padova.
- [15] M.Sakamoto, S.Kubo, T.Kubota, T.Inukai and E.Yagi, "*Optimal motorcycle configuration with performance limitations*", SAE Technical Paper, no. 2007-32-0123, 2007.
- [16] D.Tavernini, E.Velenis, R.Lot, M.Massarò, "*The Optimality of the Handbrake Cornering Technique*", ASME Journal of Dynamic Systems, Measurement and Control, 2014, vol. 136, no. 4, 041019.
- [17] D.Tavernini, M.Massarò, E.Velenis, D.I. Katzourakis, R.Lot, "*Minimum Time Cornering: The Effect of Road Surface and Car Transmission Layout*", Vehicle System Dynamics, 2013, vol.51, no. 10, pp. 1533-1547.